

AEDC-TR-90-12

UNCLASSIFIED

DOC NUM SER CN
UNC10825-PDC A 1



Infrared Surface Temperature Measurements in the Presence of Reflected Radiation

A. G. Jackson
Sverdrup Technology, Inc., AEDC Group

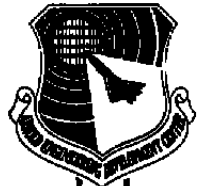
August 1990

Final Report for Period October 1988 — September 1989

Approved for public release; distribution is unlimited.

**ARNOLD ENGINEERING DEVELOPMENT CENTER
ARNOLD AIR FORCE BASE, TENNESSEE
AIR FORCE SYSTEMS COMMAND
UNITED STATES AIR FORCE**

UNCLASSIFIED



NOTICES

When U. S. Government drawings, specifications, or other data are used for any purpose other than a definitely related Government procurement operation, the Government thereby incurs no responsibility nor any obligation whatsoever, and the fact that the Government may have formulated, furnished, or in any way supplied the said drawings, specifications, or other data, is not to be regarded by implication or otherwise, or in any manner licensing the holder or any other person or corporation, or conveying any rights or permission to manufacture, use, or sell any patented invention that may in any way be related thereto.

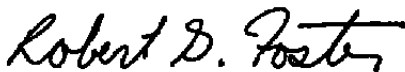
Qualified users may obtain copies of this report from the Defense Technical Information Center.

References to named commercial products in this report are not to be considered in any sense as an endorsement of the product by the United States Air Force or the Government.

This report has been reviewed by the Office of Public Affairs (PA) and is releasable to the National Technical Information Service (NTIS). At NTIS, it will be available to the general public, including foreign nations.

APPROVAL STATEMENT

This report has been reviewed and approved.



ROBERT G. FOSTER, Major, CF
Facility Technology Division
Directorate of Technology
Deputy for Operations

Approved for publication:

FOR THE COMMANDER



A. F. PHILLIPS, Lt Col, USAF
Director of Technology
Deputy for Operations

REPORT DOCUMENTATION PAGE

Form Approved
OMB No. 0704-0188

Public reporting burden for this collection of information is estimated to average 1 hour per response, including the time for reviewing instructions, searching existing data sources, gathering and maintaining the data needed, and completing and reviewing the collection of information. Send comments regarding this burden estimate or any other aspect of this collection of information, including suggestions for reducing this burden, to Washington Headquarters Services, Directorate for Information Operations and Reports, 1215 Jefferson Davis Highway, Suite 1204, Arlington, VA 22202-4302, and to the Office of Management and Budget, Paperwork Reduction Project (0704-0188), Washington, DC 20503.

1. AGENCY USE ONLY (Leave blank)		2. REPORT DATE August 1990	3. REPORT TYPE AND DATES COVERED Final -- October 1988 - September 1989	
4. TITLE AND SUBTITLE Infrared Surface Temperature Measurements in the Presence of Reflected Radiation			5. FUNDING NUMBERS PE - DB88EW	
6. AUTHOR(S) Jackson, A.G., Sverdrup Technology, Inc., AEDC Group				
7. PERFORMING ORGANIZATION NAME(S) AND ADDRESS(ES) Arnold Engineering Development Center/DOP Air Force Systems Command Arnold Air Force Base, TN 37389-5000			8. PERFORMING ORGANIZATION REPORT NUMBER AEDC-TR-90-12	
9. SPONSORING/MONITORING AGENCY NAME(S) AND ADDRESS(ES) Arnold Engineering Development Center/DO Air Force Systems Command Arnold Air Force Base, TN 37389-5000			10. SPONSORING/MONITORING AGENCY REPORT NUMBER	
11. SUPPLEMENTARY NOTES Available in Defense Technical Information Center (DTIC).				
12a. DISTRIBUTION/AVAILABILITY STATEMENT Approved for public release; distribution is unlimited.			12b. DISTRIBUTION CODE	
13. ABSTRACT (Maximum 200 words) A method is described for determining surface temperature in the presence of radiation being reflected by the surface of interest from another nearby hot surface. Radiance measurements are made on the surface of interest and on the nearby hot object in three different wavelength bands (three colors). If the emittance of the target surface varies significantly with wavelength, it is necessary to know the ratios of emittances in the three wavelength bands. An experiment was performed to demonstrate the three-color technique, and results are reported. The three-color technique was shown to be highly sensitive to non-gray behavior. Application of the three-color technique with corrections for non-gray behavior resulted in temperature measurement errors less than 2 percent in the presence of reflected radiation. Conventional ratio pyrometry (two colors) resulted in errors greater than 10 percent in the presence of reflected radiation.				
14. SUBJECT TERMS optical pyrometry surface temperature ratio pyrometry			15. NUMBER OF PAGES 52	
			16. PRICE CODE	
17. SECURITY CLASSIFICATION OF REPORT UNCLASSIFIED		18. SECURITY CLASSIFICATION OF THIS PAGE UNCLASSIFIED	19. SECURITY CLASSIFICATION OF ABSTRACT UNCLASSIFIED	20. LIMITATION OF ABSTRACT SAME AS REPORT

PREFACE

The work reported herein was conducted by the Arnold Engineering Development Center (AEDC), Air Force System Command (AFSC), under Program Element 65807F. The results were obtained under Sverdrup Project No. DB88 by Sverdrup Technology, Inc., AEDC Group (a Sverdrup Corporation Company), operating contractor for the engine test facilities at AEDC, AFSC, Arnold Air Force Base, Tennessee. The Air Force Project Manager was Major Robert G. Foster (CF), AEDC/DOTR. The manuscript was submitted for publication on June 29, 1990.

CONTENTS

	<u>Page</u>
1.0 INTRODUCTION	5
2.0 APPARATUS	6
2.1 Infrared Radiation Detection System	6
2.2 Target Surface	8
2.3 High-Temperature Radiation Source	10
3.0 PROCEDURE	11
3.1 Problem Statement	11
3.2 Three-Color Theory	12
3.3 Surface and Radiometer Calibrations	14
3.4 Setup and Data Acquisition	15
3.5 Data Reduction	15
4.0 RESULTS	17
4.1 Results with Gray-Body Assumption	17
4.2 Results with Estimated Values for Emittance	18
4.3 Results with Measure Emittance Values	19
5.0 CONCLUSIONS AND RECOMMENDATIONS	20
5.1 Conclusions	20
5.2 Recommendations	21
REFERENCES	22

ILLUSTRATIONS

<u>Figure</u>	<u>Page</u>
1. Barnes® Spectral Master Radiometer	25
2. Barnes Radiometer Detector Spectral Response	26
3. Internal View of Barnes Spectral Master Radiometer	27
4. Water Vapor and Carbon Dioxide Absorbtion and Emission Bands in the 1.5- to 4.5- μ m Range	28
5. Electrically Heated Target Surface	29
6. Comparison of Specular and Diffuse Reflections	30
7. Target Surface Reflection Characteristics before and after Surface Treatments	31
8. Aluminum Target Surface with Dimples	32
9. Total Emittance of an Aluminum Plate (Typical Published Values)	33

<u>Figure</u>	<u>Page</u>
10. Spectral Emittance of Aluminum at Room Temperature (Typical Published Values)	33
11. Photograph of 1-in. Blackbody Radiator	34
12. Radiosity (B)	35
13. Single-Color Calibrations	35
14. Radiance Ratios	36
15. Target Surface Temperature Profiles and Correction to Imbedded Thermocouple Readings	37
16. Target Temperature Stability During Three-Color Experiment	38
17. Hardware Setup for Three-Color Experiment	38
18. Geometry Factor (g) Convergence Leading to Three-Color Solutions	39
19. Comparison of Calculated Temperature Errors with Increasing Reflected Radiant Energy (Gray-Body Assumption)	40
20. Comparison of Calculated Temperature Errors with Increasing Reflected Radiant Energy (Using Published Values for Emittance)	41
21. Comparison of Calculated Temperature Errors with Increasing Reflected Radiant Energy (Using Measured Values for Emittance)	42

TABLES

<u>Tables</u>	<u>Page</u>
1. List of Filters Installed in Barnes Radiometer	43
2. Tabulated Radiance Ratios from 300 to 500°C	44
3. Estimated Contributors to Target Surface Temperature Uncertainty	48
4. Summary of Single-Color, Two-Color, and Three-Color Solutions with Gray-Body Assumption	48
5. Summary of Single-Color, Two-Color, and Three-Color Solutions with Published Values for Emittance	49
6. Summary of Single-Color, Two-Color, and Three-Color Solutions with Measured Values for Emittance	49

1.0 INTRODUCTION

Infrared pyrometry is used as a nonintrusive temperature measurement technique where high temperatures are involved and where environmental factors render conventional temperature measurement techniques (i.e., thermocouples, thermistors, etc.) of limited use. The infrared pyrometry technique, however, can result in significant measurement errors if the emissive properties of the surface are not well known and if the surface of interest is reflecting radiation from another source.

Surface temperature measurements using infrared techniques are subject to error if the area of interest (target) is reflecting radiation from a hotter source. The magnitude of this temperature error is a function of the temperature ratio between the target and the hotter source, the view factor between them, and the spectral surface properties of the target and the hotter source.

Infrared temperature measurement techniques calculate surface temperature from detected surface radiation. The total amount of radiation reaching the detector will be proportional to the radiosity (B) of the target, and will be a function of the optical path, target emissivity, and geometry of the instrument. The radiosity is the rate at which energy streams away from the target surface and is the sum of the radiance (energy emitted by the surface), $\int \epsilon E_b(\lambda, T) d\lambda$, and the reflected incident radiation (ρH), where $E_b(\lambda, T)$ is the spectral emissive power of a blackbody at a given wavelength (λ) and temperature (T), and H is the spectral incident radiant energy from all sources. Emissivity (ϵ) plus hemispherical reflectivity (ρ) equal unity for an opaque surface at equilibrium (constant temperature). For an approximate temperature calculation based on infrared measurements, ϵ can be estimated or assumed to be 1.0 and reflections are usually neglected. When measurements are taken over a narrow wavelength band ($(\lambda_b - \lambda_a) \ll 1.0 \mu\text{m}$), the radiance may be assumed to be a constant over the wavelength band of the measurement, eliminating the need for integration. The surface temperature can then be calculated from the relation $B = k\epsilon E_b(\lambda, T)$ where k is a function of instrument sensitivity and is determined by calibration. Measurements made over a single wavelength band will be referred to hereafter as single-color measurements. Note that single-color measurements are subject to error if the true emissivity is not known or if significant amounts of incident radiation are present.

By measuring the radiosity in two different wavelength bands (two-color method), reliance on a correctly known value for emittance is eliminated, assuming gray-body behavior (i.e., ϵ does not vary with wavelength). The two-color method is described in Ref. 1. The two-color method, however, is also subject to error if significant amounts of incident radiation are present.

The objective of the experiment reported herein is to demonstrate a surface temperature measurement technique that will not require prior knowledge of the surface properties and will correct for errors that may be introduced by the presence of radiation originating from a source hotter than the target. The technique uses a radiometer with filters at three different wavelength bands (three colors) and will be referred to hereafter as the three-color technique or three-color method. The information gathered through such measurements should be sufficient to formulate a correction to the measured surface temperature to account for the reflected radiation from a hotter surface. Absolute temperature measurements within ± 5 percent are desired [$\pm 30^\circ\text{C}$ at 350°C (623 K)].

The three-color method assumes that the surface to be measured is gray and diffuse. It also assumes that all of the energy incident on the target can be considered to emanate from a single source. It is recognized that these assumptions may not be valid for all applications, but these assumptions are made to simplify the investigation of the three-color technique and determine whether further investigation is warranted.

This demonstration of the three-color technique uses a simple flat-plate geometry. The target surface is a heated aluminum plate that has been instrumented with thermocouples to determine an indicated bulk metal temperature. True target surface temperature will be considered to be the bulk metal temperature adjusted for a temperature gradient across the thickness of the plate. Blackbody radiation is used as a source of reflected energy, providing incident radiation at 900°C and at $1,000^\circ\text{C}$. Single-color, two-color, and three-color radiometric surface temperature solutions for the target surface are compared.

2.0 APPARATUS

The apparatus used in this experiment is comprised of three major components: an infrared radiation detection system (radiometer), a heated target surface, and a high-temperature radiation source of incident energy.

2.1 INFRARED RADIATION DETECTION SYSTEM

The infrared radiation detection system chosen for this investigation was a Barnes® Spectral Master Radiometer, Model 12-660, Serial Number 119, manufactured by Barnes Engineering Co., 30 Commerce Rd., Stamford, CT. The Barnes radiometer was chosen because it incorporates a remotely controlled eight-position filter wheel (the ability to detect radiation in at least three discrete wavelength bands was critical in this experiment), it is considered simple and reliable, and it uses a variable gain amplifier which gives the instrument a large measurement range. The Barnes radiometer incorporates an immersed thermistor bolometer detector with an anti-reflection-coated germanium lens. Operating principles of the thermistor bolometer are described in Ref. 2.

2.1.1 Radiometer Characteristics

The Barnes radiometer is shown in Fig. 1. The bolometer detector spectral response is 1.8 to 28 μm (Fig. 2). An eight-position filter wheel is mounted in front of the detector (Fig. 3). The filter wheel is driven by a remotely controlled stepper motor. A lens-holding fixture is located in front of the filter wheel. No lens was installed during the three-color experiment. A chopper wheel is located in front of the lens holder, providing a square wave chopping function at 15 Hz. The front end of the radiometer has a removable cover with a rectangular aperture measuring 1 by 1.75 in.

The field of view (FOV) of the radiometer as configured for the experiment was determined to be approximately 20 deg in the horizontal direction. The vertical FOV was not measured, but because the bolometer lens is spherical and the filters are circular, the vertical FOV is assumed to be approximately equal to the horizontal FOV. The radiometer cover plate does not restrict the FOV. The FOV is important primarily to help determine target spot size, and to ensure that the FOV is filled during portions of the radiometer calibration process.

2.1.2 Filters

The Barnes radiometer filter wheel can accommodate up to eight 0.35-in.-diam filters. Seven filters were installed, leaving one filter position open. The choice of filters for this experiment was influenced by filter suitability and availability.

Filter suitability is a function of the temperature of the surface that is being measured, the response of the instrument, and the requirement to avoid the CO_2 and H_2O emission and absorption bands (Fig. 4). For this investigation, the surface temperature range was limited to 300 to 600°C by the capabilities of the heated target surface (see Section 2.2). The three-color temperature measurement technique requires the measurement of radiant energy at three discrete wavelengths that will result in three distinct and usable radiance ratios. If the center wavelength and the bandwidth of each filter is selected such that the energy collected in each wavelength band is of the same order of magnitude, the radiance ratios can be computed directly from the measured radiometer response (mv). Energy levels that are not of the same order of magnitude may lead to radiance ratios with significant round-off errors. Using calculated in-band radiance to determine radiance ratio may obviate the requirement to select filters with similar total bandpass energy levels, but for the sake of simpler data reduction, comparable total bandpass energy levels were considered a requirement for the filters selected.

Filter availability was also a factor considered, since the selection of filters sized to fit the filter wheel (0.35-in. diam) was limited. Filters were chosen from among those already available through commercial suppliers. They were installed in the filter wheel as shown in Table 1.

2.2 TARGET SURFACE

The target surface was designed to produce the best experimental results possible using readily available materials. The primary features that were considered important for the target surface were stable temperature control, uniform surface temperature, independent temperature verification, diffuse surface behavior, and an emittance level significantly less than 1.0. An electrically heated aluminum plate was chosen for the target surface. The properties of the aluminum plate did not meet the specifications in all cases, but were believed to provide a reasonable approximation within the available resources. A sketch of the target is shown in Fig. 5, and the target's properties are discussed below.

2.2.1 Target Temperature Control

Target temperature was controlled using an electric hotplate with a variable power supply. Supply voltage could be varied between 30 and 120 vAC. The hot-plate was made of cast iron with resistance heater coils located behind the cast-iron plate. The hotplate temperature at 120 v stabilized at approximately 500°C. The cast-iron surface of the hotplate exhibited an emittance very close to 1.0 and was therefore considered unsuitable for this experiment. An aluminum plate was bolted to the hotplate to serve as the target surface. The high thermal conductivity of the aluminum provided good heat transfer from the hotplate. Observation of the stabilization temperature after the addition of the aluminum plate indicated that the aluminum surface actually stabilized at a higher temperature than the cast iron surface did prior to the addition of the aluminum plate. This is believed to be attributable to the lower emissivity of aluminum.

2.2.2 Uniform Surface Temperature

Uniform target surface temperatures were important to the successful completion of this experiment. It was expected that the edges of the target would be slightly cooler than the center. Aluminum was chosen for the target surface partly for its high thermal conductivity, which was expected to minimize radial temperature gradients. A circular target would be preferred to a square or rectangular target from the standpoint of minimizing circumferential temperature gradients attributable to radiation from the four corners, but for ease of fabrication, an octagonal shape was chosen. A Hughes Probeye® camera was used to check the radial and circumferential temperature profiles. Surface-mounted thermocouples were added to further assess temperature gradients, but they were not installed when radiance readings were taken. Target surface temperature gradients are discussed in Section 3.3.2.

2.2.3 Independent Temperature Verification

Independent verification of the target surface temperature is required for the validation of the three-color temperature measurement technique. Installation of thermocouples directly on the target surface helped assess surface temperatures, but was not considered feasible during radiance measurements because the thermocouples would interfere with the radiance readings. Internal thermocouples were imbedded at four locations around the plate (see Fig. 5). Digital readout of the thermocouples was used to provide an indication of the surface temperature. The Hughes Probeye data and data from the surface-mounted thermocouples were used to formulate an adjustment to the indicated temperature (from the imbedded thermocouples) to provide the best possible estimate of target true surface temperature (hereafter referred to as T_{true}). (Further discussion of this temperature adjustment is found in Section 3.3.2). It must be emphasized that throughout this discussion, references to T_{true} are used for convenience in making comparisons. In reality, T_{true} cannot be represented by a single number but as a temperature band within which the true target surface temperature is believed to fall. This temperature band (uncertainty) is estimated to be $\pm 5^{\circ}\text{C}$.

2.2.4 Diffuse Surface Behavior

The three-color surface temperature measurement technique assumes but does not require diffuse behavior. Most surfaces of interest are probably more diffuse than specular. In a specular reflector, the angle of incidence is equal to the angle of reflection. A diffuse reflector reflects equally in all directions (Fig. 6). Any real surface will have some diffuse and some specular reflection. A polished surface is usually predominantly specular, while a dull, rough, or oxidized surface will generally be more diffuse. The intent of this experiment was to develop a temperature measurement technique that might be used with predominantly diffuse surfaces; therefore, a predominantly diffuse target was desired. The target surface was made from smooth, unpolished aluminum. An experiment was conducted with the aluminum plate to estimate how specular the surface was. Incident radiation was directed at the surface at an angle of 50 deg from the surface. Radiance readings were made from the target at angles from 30 to 90 deg. The untreated surface showed a high specular reflection contribution as indicated by high readings at 50 deg (Fig. 7). The surface was roughened using No. 150 emery paper, and the readings were repeated. The specular reflection was reduced significantly. A surface dimpling technique was used to introduce a pattern of dimples approximately 1 mm in diameter and 0.5 mm deep in the target surface (Fig. 8). The dimples act as many small cavity radiators on the surface and have the effect of reducing the specular component of the reflection. The reflection experiment showed that the specular reflection after dimpling was sharply reduced from that of the untreated surface (Fig. 7).

2.2.5 Emittance Level

Emissivity (ϵ) is a material property that relates how a material emits radiation relative to a perfect emitter (blackbody, $\epsilon = 1.0$). Reflectivity is the property that relates how a material reflects radiation relative to a perfect reflector (white surface, $\rho = 1.0$). While the terms "emittance" and "emissivity" are sometimes used interchangeably and are denoted by the same symbol (ϵ), the term "emittance" in this discussion refers to the emissive properties of a particular specimen rather than a material. Similarly, "reflectance" (ρ) refers to the reflective properties of a particular specimen. An emittance level between 0.5 and 0.8 was desired for this experiment. An estimate of the emittance of a smooth, unpolished aluminum surface obtained from published sources (Ref. 6.) is shown in Fig. 9. Notice that the total emittance of aluminum increases slightly with surface temperature. The change of emittance with a change in surface temperature introduces an error in a single-color radiance measurement, but if the emittance ratio remains constant, emittance changes with temperature should not be a source of error in multi-color measurements (two-color and three-color methods). Note however, that at a temperature near 500°C, the total emittance is estimated to be approximately 0.1, far below the desired level for this experiment.

An estimate of the spectral emittance for aluminum at room temperature is shown in Fig. 10. Notice that emittance varies with wavelength. This represents a source of error for the multi-color measurement. For this experiment, the emittance is desired to be constant at wavelengths from 2 to 4 μm . A discussion of ways to account for errors attributable to emittance variation with wavelength (non-gray behavior) is presented in Section 3.5.

2.3 HIGH-TEMPERATURE RADIATION SOURCE

A high-temperature source of radiation was required to provide reflected energy for the demonstration of the three-color temperature measurement technique. The high-temperature source provided radiation incident on the target surface. Such incident radiation on the target surface, reflected into the radiometer, can cause temperature errors in the single-color and two-color measurements, and it motivated the proposal of the three-color method. The source of the incident radiation for this experiment does not need to be diffuse or gray if direct readings can be taken with the radiometer. To simplify the experiment, a pair of 1-in. blackbodies was selected as the source of the high-temperature radiation (Fig. 11). The use of blackbodies for the source of high-temperature incident radiation in this experiment eliminated the need to take direct measurements from the high-temperature surface.

3.0 PROCEDURE

3.1 PROBLEM STATEMENT

Surface temperature measurements using infrared techniques are subject to error if the area of interest (target) is reflecting radiation from a hotter source. The magnitude of this error is a function of the temperature ratio between the target and the hotter source, the view factor between them, and the spectral surface properties of the target and the hotter source.

Infrared temperature measurement techniques determine surface temperature by measuring the radiation from the target surface. The total amount of radiation reaching the detector will be proportional to the radiosity (B) of the target and will be a function of the optical path, target emissivity, and geometry of the instrument. The radiosity is the rate at which energy streams away from the target surface and is the sum of the radiance (energy emitted by the surface) $\int \epsilon E_b(\lambda, T) d\lambda$ and the reflected incident radiation (ρH) (Fig. 12). The term ρH represents the incident radiation on the target surface that is reflected into the radiometer. Traditional infrared temperature measurement techniques assume that ρH is negligible. If the magnitude of ρH is significant relative to the magnitude of $\int \epsilon E_b(\lambda, T) d\lambda$, a significant error will result in the infrared surface temperature measurement.

For a temperature calculation based on infrared measurements in a single wavelength band and with no reflected radiation, ϵ can be assumed to be some value ≤ 1.0 and ρH is zero. For measurements taken over a narrow wavelength band ($(\lambda_b - \lambda_a) \ll 1.0 \mu\text{m}$) the radiance may be assumed to be a constant over the wavelength band of the measurement, eliminating the need for integration. The surface temperature can then be calculated from the relation $V = kE_b(\lambda, T)$ where k is a function of instrument sensitivity and is determined by calibration and V is the instrument reading. Measurements made over a single wavelength band are referred to as single-color measurements. Note that single-color measurements are subject to error if the true value of the emittance is not known or if incident radiation is present.

By measuring the radiosity in two different wavelength bands (two-color method), reliance on a correctly known value for emittance is eliminated (assuming gray-body behavior). The two-color method is described in Ref. 1. Atkinson and Strange have also done extensive work using a two-color method to determine aircraft turbine blade temperatures in the presence of reflected radiation (Refs. 3 and 4). They have proposed several methods of improving the accuracy and utility of their two-color method. Among their recommended approaches is a multi-color method, although no specifics are mentioned. Multi-color methods have been explored for determining surface temperatures of molten gas-tungsten arc weld pools (Ref. 5). This approach uses up to 500 measurements at discrete wavelength bands between 0.60 and 0.80 μm . This method, however, assumes that only emitted radiation is being measured.

This review of current IR pyrometry practices points out the need for an improved radiometric technique that can, without detailed knowledge of surface emittances, be applied to the measurement of hot surfaces that may also be reflecting energy from another source.

3.2 THREE-COLOR THEORY

This work proposes a three-color infrared measurement technique for determining surface temperature using a radiometer with filters at three different wavelength bands (three colors). The information gathered through such measurements is sufficient to formulate a correction to the measured surface temperature to account for reflected radiation from a hotter surface. The three-color approach assumes that the surface to be measured is gray and diffuse. It is also assumed that all of the energy incident on the target can be considered to emanate from a single source.

The radiosity (B1) from the target (surface 1) in the presence of reflection from another hot surface (surface 2) measured in three different wavelength bands is:

$$B1\lambda_1 = \epsilon\lambda_1 Eb(\lambda_1, T1) + (1-\epsilon\lambda_1) F_{1-2} B2\lambda_1 \quad (1)$$

$$B1\lambda_2 = \epsilon\lambda_2 Eb(\lambda_2, T1) + (1-\epsilon\lambda_2) F_{1-2} B2\lambda_2 \quad (2)$$

$$B1\lambda_3 = \epsilon\lambda_3 Eb(\lambda_3, T1) + (1-\epsilon\lambda_3) F_{1-2} B2\lambda_3 \quad (3)$$

where B1 and B2 are the radiosities of surface 1 and 2, ϵ is the emittance of surface 1, F_{1-2} is the shape factor between surface 1 and surface 2, and $Eb(\lambda, T1)$ is the spectral emissive power of a blackbody at temperature T1 and wavelength λ . The radiosities of surface 1 and surface 2 at the three wavelengths can be determined by radiance measurements made in the three wavelength bands. If we assume that surface 1 behaves as a gray body ($\epsilon\lambda_1 = \epsilon\lambda_2 = \epsilon\lambda_3 = \epsilon$), this leaves three equations in three unknowns (F_{1-2} , ϵ , and $Eb(\lambda, T1)$) which can be solved to yield T1. However, since T1 is implicit in $Eb(\lambda, T1)$, the solution is not straightforward. The following solution is proposed.

By algebraic manipulation, Eqs. (1), (2), and (3) can be rewritten in the form:

$$\frac{Eb(\lambda_1, T1)}{Eb(\lambda_2, T1)} = \frac{B1\lambda_1 - gB2\lambda_1}{B1\lambda_2 - gB2\lambda_2} = R_{12} \quad (1a)$$

$$\frac{Eb(\lambda_1, T1)}{Eb(\lambda_3, T1)} = \frac{B1\lambda_1 - gB2\lambda_1}{B1\lambda_3 - gB2\lambda_3} = R_{13} \quad (2a)$$

$$\frac{Eb(\lambda_2, T1)}{Eb(\lambda_3, T1)} = \frac{B1\lambda_2 - gB2\lambda_2}{B1\lambda_3 - gB2\lambda_3} = R_{23} \quad (3a)$$

where g is a geometry factor ($g = (1-\epsilon) F_{1-2}$)

This now represents three equations describing the blackbody radiance ratios of surface 1 at the true temperature computed at the specified wavelengths. There are four unknowns (g , R_{12} , R_{13} , and R_{23}) in Eqs. (1a), (2a), and (3a), but R_{12} , R_{13} , and R_{23} are functions of T_1 . The relationship between these ratios (R_{12} , R_{13} , and R_{23}) and T_1 is determined through calibration with a blackbody. Three solutions for geometry factor (g) can be derived from Eqs. (1a), (2a), and (3a), yielding the following three expressions:

$$g_1 = \left(\frac{R_{12}B_1\lambda_2 - B_1\lambda_1}{R_{12}B_2\lambda_2 - B_2\lambda_1} \right) \quad (1b)$$

$$g_2 = \left(\frac{R_{13}B_1\lambda_3 - B_1\lambda_1}{R_{13}B_2\lambda_3 - B_2\lambda_1} \right) \quad (2b)$$

$$g_3 = \left(\frac{R_{23}B_1\lambda_3 - B_1\lambda_2}{R_{23}B_2\lambda_3 - B_2\lambda_2} \right) \quad (3b)$$

Now if the gray-body assumption is true, then $g_1 = g_2 = g_3$ and hence:

$$\left(\frac{R_{12}B_1\lambda_2 - B_1\lambda_1}{R_{12}B_2\lambda_2 - B_2\lambda_1} \right) - \left(\frac{R_{13}B_1\lambda_3 - B_1\lambda_1}{R_{13}B_2\lambda_3 - B_2\lambda_1} \right) = 0 \quad (4a)$$

$$\left(\frac{R_{12}B_1\lambda_2 - B_1\lambda_1}{R_{12}B_2\lambda_2 - B_2\lambda_1} \right) - \left(\frac{R_{23}B_1\lambda_3 - B_1\lambda_2}{R_{23}B_2\lambda_3 - B_2\lambda_2} \right) = 0 \quad (4b)$$

$$\left(\frac{R_{13}B_1\lambda_3 - B_1\lambda_1}{R_{13}B_2\lambda_3 - B_2\lambda_1} \right) - \left(\frac{R_{23}B_1\lambda_3 - B_1\lambda_2}{R_{23}B_2\lambda_3 - B_2\lambda_2} \right) = 0 \quad (4c)$$

All of the parameters in Eq. (4a) are known except the radiance ratios R_{12} , R_{13} , and R_{23} . They are implicit functions of the single unknown T_1 . For a given value of T_1 , corresponding values of R_{12} , R_{13} , and R_{23} have been determined from the blackbody calibration. Equation (4a) can be solved iteratively by assuming a value for T_1 which then determines R_{12} , R_{13} , and R_{23} . A non-zero result of Eq. (4a) indicates that the assumed value for T_1 was in error. By raising or lowering T_1 and solving iteratively, Eq. (4a) can be made to converge on a solution close to zero (See Section 3.5). T_1 at the point of convergence is the three-color solution for T_1 . Solutions for Eqs. (4b) and (4c) can be derived similarly. In the ideal case, the solutions of Eqs. (4a),(4b), and (4c) will yield a single value for T_1 . When real data are used, each solution may yield a slightly different value for T_1 . Unless otherwise specified in the discussion that follows, the three-color temperature solution will be represented by the average of the three values derived for T_1 from Eqs. (4a), (4b), and (4c).

3.3 SURFACE AND RADIOMETER CALIBRATIONS

3.3.1 Radiometer Calibration

The Barnes radiometer was calibrated for all eight filter positions using a 6-in. blackbody (B.B.) from 200° to 500°C (the maximum temperature achievable). The 6-in. B.B. was chosen to ensure that the radiometer FOV would be filled. A filled FOV is a requirement for single-color calibration. The single-color calibration consisted of establishing a millivolt versus B.B. temperature relationship at six temperature intervals for the radiometer at each filter setting (Fig. 13). The six calibration points were used to produce calibration curves of the form millivolts = a(T)^x.

Radiance ratio (two-color) calibrations were determined by calculating the ratio of the single-color readings in different wavelength bands (filter settings). With radiometer readings using eight different filters (the open position with no filter can be treated as a filter with 100-percent bandpass over the total range of the radiometer spectral response), 28 unique ratio combinations may be formed. Of these ratio combinations, the three that appeared to be best suited to the three-color method in the temperature range of this experiment were from filter 2 (2.0 - 2.4 μm), filter 3 (3.4 - 3.6 μm), and filter 5 (3.8 - 4.0 μm). These three filters were then chosen for the three-color experiment and are designated as λ₁, λ₂, and λ₃ throughout the rest of this discussion (i.e., filter 2 = λ₁, filter 3 = λ₂, and filter 5 = λ₃). The radiance ratios with these three filters (Fig. 14) are calculated with the shorter wavelength in the numerator:

$$R_{12} = \left(\frac{\lambda_1 \text{ radiance}}{\lambda_2 \text{ radiance}} \right) = \left(\frac{\text{mv reading w/ filter 2}}{\text{mv reading w/ filter 3}} \right)$$

$$R_{13} = \left(\frac{\lambda_1 \text{ radiance}}{\lambda_3 \text{ radiance}} \right) = \left(\frac{\text{mv reading w/ filter 2}}{\text{mv reading w/ filter 5}} \right)$$

$$R_{23} = \left(\frac{\lambda_2 \text{ radiance}}{\lambda_3 \text{ radiance}} \right) = \left(\frac{\text{mv reading w/ filter 3}}{\text{mv reading w/ filter 5}} \right)$$

Second-order curve fits of the six calibration points were used to generate radiance ratio tables from 200° to 500°C (Table 2).

3.3.2 Target Surface Calibration

Four thermocouples were imbedded in the aluminum target to provide an independent indication of surface temperature (See Section 2.2.3). Surface-mounted thermocouples were also added to help determine the magnitude of radial surface temperature profiles and to

derive an adjustment to the imbedded thermocouple readings to provide the most accurate surface temperature indication that was possible. High emissivity black paint was applied to a small spot located away from the target area. A Hughes Probeye camera temperature determination of black spot temperature agreed within 2 percent of the surface-mounted thermocouple at the center of the target with the target heated to 500°C. Radial surface temperature profiles are shown in Fig. 15a. The radiometer FOV produced a target spot size with a radius of approximately 1.5 in. The radial profile within this radius was estimated to be small enough ($\leq 1^\circ\text{C}$) to be ignored in the calculation of target surface temperature. A correlation between the indicated black spot temperature internal thermocouple reading at 0 deg (12 o'clock position) was used to formulate a calculation of the surface temperature based on the internal thermocouple reading. An adjustment of 3°C is applied to this thermocouple reading to give an estimate of the surface temperature in the center of the target (see Fig. 15b). The indicated target surface temperature remained stable within $\pm 1^\circ\text{C}$ throughout the experiment (Fig. 16). Anticipated contributors to surface temperature uncertainty are listed in Table 3. The total surface temperature uncertainty is estimated to be $\pm 5^\circ\text{C}$.

3.4 SETUP AND DATA ACQUISITION

The setup for the three-color experiment is shown in Fig. 17. The radiometer was positioned 6 in. from the target surface. The small distance between the radiometer and the target was required to keep the target spot size to a minimum ($\approx 3\text{-in. diam.}$). The two blackbody radiators were also located about 6 in. from the target surface at an angle of about 45 deg on each side of the radiometer. One of the blackbodies produced a lower intensity reflection than the other one, despite the fact that they were set to the same temperature. This difference in reflected energy is attributed to slight differences in alignment of the blackbodies or to surface irregularities. This resulted in three different reflected energy levels when the blackbodies were opened and closed in combination. Blackbody A by itself yielded the lowest intensity (≈ 5 percent at 1,000°C). Blackbody B yielded an intensity nearly double that for Blackbody A (≈ 10 percent at 1,000°C). The intensities were additive when both blackbodies were open (≈ 15 percent at 1,000°C). The percent reflected energy (percent reflection) was calculated as shown below:

$$\text{percent reflection} = \left(\frac{\text{total energy with reflection}}{\text{total energy with no reflection}} - 1.0 \right) \times 100$$

3.5 DATA REDUCTION

Reduction of the experimental data was accomplished using a simple computer program. Raw millivolt readings and corresponding attenuation values were combined with the

appropriate zero offset to yield adjusted millivolt readings for each wavelength band (filter position) where data were collected. The adjusted millivolt values were divided by the assumed value for emittance and compared to the single-color calibration curves to determine single-color temperature solutions.

Radiance ratios calculated from the adjusted millivolt values were compared to tabulated radiance ratio versus temperature data from the radiometer calibration. In this way, two-color temperatures were computed. The two-color temperature solutions are denoted T_{12} , T_{13} , and T_{23} calculated from R_{12} , R_{13} , and R_{23} , respectively.

Values for the geometry factor (g) were calculated for R_{12} , R_{13} , and R_{23} as outlined in Section 3.2 [Eqs. (1b), (2b), and (3b)]. An example of these solutions is shown graphically in Fig. 18. In the ideal case, convergence of the three values of g at a single point indicates the three-color temperature solution. But in an example with real data, the three curves representing the g values intersect at three different points, yielding three different solutions. These three solutions will be denoted T_1 [Eq. (4a), Section 3.2], T_2 [Eq. (4b)], and T_3 [Eq. (4c)].

The single-color, two-color, and three-color temperature measurement techniques each yield three solutions when the data from three wavelength bands are used. Unless otherwise noted in the following discussion, an average of the three solutions resulting from the three wavelengths will be used to represent the solution for each of the measurement techniques.

The two-color and three-color solutions are based on the assumption that the surface being measured behaves as a gray body. If gray-body behavior is not assumed, a correction to the radiance ratios can be made:

$$R_{12 \text{ calibration}} = \left(\frac{E_b(\lambda_1, T)}{E_b(\lambda_2, T)} \right)$$

$$R_{12 \text{ measured}} = \left(\frac{\epsilon_1 E_b(\lambda_1, T)}{\epsilon_2 E_b(\lambda_2, T)} \right)$$

$$R_{12 \text{ calibration}} = R_{12 \text{ measured}} \times \left(\frac{\epsilon_2}{\epsilon_1} \right)$$

4.0 RESULTS

4.1 RESULTS WITH GRAY-BODY ASSUMPTION

The objective of the three-color measurement technique is the determination of surface temperature in the presence of reflected radiation without prior information about surface properties. The two-color and three-color methods do not require knowledge of emittance values, but emittance ratios must be known. This is not a problem if the target surface properties approximate those of a gray body, for then the emittance ratios are known to be approximately 1.0. The assumption of gray-body behavior does not stipulate specific values for ϵ_1 , ϵ_2 , or ϵ_3 . For single-color data reduction, the emittances were assumed to be 1.0. The temperature solutions for each of the three methods discussed are presented in Table 4. The estimated temperature errors are compared in Fig. 19.

4.1.1 Single-Color Solutions with Gray-Body Assumption

The estimated error of the single-color solution with the gray-body assumption and ϵ assumed equal to 1.0 (Fig. 19), even without reflection is substantial (-50°C). This is, of course, because the actual values of ϵ were not used in the data reduction. (No *a priori* information is assumed other than graybody behavior.) Note, however, that as reflected energy increases, the single-color error decreases. This result could have been anticipated since the effect of incident radiation is to increase the indicated single-color temperature, and the assumption $\epsilon = 1.0$ causes indicated single-color temperature to err on the low side of T_{true} . However, it must be noted that at some level of reflected energy, the indicated single-color temperature will reach T_{true} and at that point further increases in reflected energy will increase the single-color temperature errors. Since the reflected energy in the typical experiment is neither controlled or known, it is difficult to assess from the single-color data whether or not this point has been reached. Still, it is important to observe that the single-color errors in this experiment decrease as reflected energy increases.

4.1.2 Two-Color Solutions

The two-color solution errors are also presented in Fig. 19. Note that the two-color error is over 60°C with no reflection. This is, no doubt, a result of the incorrect assumption of gray-body behavior. As with the single-color solutions, the two-color solution indicates higher surface temperatures with reflected energy. But since the two-color solution initially errs on the high side of T_{true} , the two-color temperature errors increase with increasing reflected energy. Notice also that the slope of the line through the two-color solution errors is greater than that through the single-color errors. This indicates that the two-color solution is more sensitive to error from reflected energy than the single-color solution.

4.1.3 Three-Color Solution

The three-color solution with no reflected energy yields approximately the same error as the two-color solution. This is expected, since the three-color solution with no reflected radiation reduces to the two-color solution. (No reflection implies that $\rho F_{1-2} = g = 0$.) The three-color solution errors decrease with increasing reflected energy. This is a fortuitous result arising from the fact that the solution with no reflection errs on the high side of T_{true} . The magnitudes of the three-color temperature errors are significantly higher than those proposed for validation of the three-color method. The data suggest that the gray-body assumption is not valid for this experiment.

4.2 RESULTS WITH ESTIMATED VALUES FOR EMITTANCE

The assumption that the target surface was a good approximation of a gray surface was questioned after reviewing the properties of aluminum in published sources. However, the surface properties of aluminum are so highly variable (dependent on surface preparation, smoothness, oxidation, etc.) that a reasonable estimate for the spectral emittance of the target surface was difficult to obtain. Additionally, the target surface in this experiment has a unique surface treatment (dimples) that has been shown to have a dramatic effect on the room temperature surface properties. Fortunately, the two-color method and the three-color method do not require specific values for spectral emittance, but rather the ratio of emittance in the wavelength bands of interest must either be known or assumed. Emittance estimates of $\epsilon_1 = 0.166$, $\epsilon_2 = 0.099$, and $\epsilon_3 = 0.088$ were obtained for smooth, unpolished aluminum from Ref. 6 (see Section 2.2.5). The results of data reduction using the emittance values are presented in Table 5. The single-color, two-color, and three-color measurement errors are compared in Fig. 20.

4.2.1 Single-Color Solution with Published Emittance Estimate

The single-color solutions with the estimated emittances from Ref. 6 yield temperatures on the high side of T_{true} . The estimated emittances are, no doubt, too low for this target surface as anticipated. Note that the single-color temperature errors using the published emittance estimates increase with increasing reflected energy. The sensitivity of the single-color temperature solutions to the percent reflected energy is about the same using the estimated values for emittance as for the solutions with graybody assumption, but the magnitude of the errors is much greater.

4.2.2 Two-Color Solution with Published Emittance Estimates

The use of published emittance estimates in the two-color solution reduces the errors dramatically when they are compared with the solution with graybody assumption. The error

with no reflection is about -25°C and decreases to 0°C at 8-percent reflected energy before increasing to $+30^{\circ}\text{C}$ at 15-percent reflected energy. The two-color solution using the published emittance estimates remains sensitive to reflected energy.

4.2.3 Three-Color Solution with Published Emittance Estimates

The three-color solution errors with the published emittance estimates range from -40°C with no reflection to over -50°C with 15-percent reflected energy. This is not a significant improvement over the three-color solutions with the gray-body assumption. Note that in this case the measurement error is increasing with increasing reflected energy.

The magnitude of the three-color temperature errors remains significantly higher than those proposed for validation of the three-color method. The data suggest that the three-color method is not valid for this experiment using estimated values of emittance obtained from Ref. 6.

4.3 RESULTS WITH MEASURED EMITTANCE VALUES

Estimates for the spectral emittance of the aluminum target can be made using the single-color data with no reflections. These estimates of emittance using experimental data will be referred to as measured emittance values. They are calculated by dividing the measured millivolt reading by the calibration millivolt reading at T_{true} :

$$\epsilon_1 = \frac{\text{mv } \lambda_1 \text{ (measured with no reflection)}}{\text{mv } \lambda_1 \text{ (from calibration curve at } T_{\text{true}})}$$

Measured values for ϵ_2 and ϵ_3 are calculated in similar fashion. Temperature solutions using these measured values for emittance ($\epsilon_1 = 0.685$, $\epsilon_2 = 0.483$, and $\epsilon_3 = 0.452$) are presented in Table 6. A comparison of the temperature measurement errors for the three methods using measured emittance is presented in Fig. 21.

4.3.1 Single-Color Solutions with Measured Emittance

These estimates for emittance, by nature of their derivation from the data with no reflection and T_{true} , will cause the single-color measurement error with no reflection to approach zero. The single-color measurements are still subject to increasing error with increasing reflected energy; however, the errors remain $\leq 10^{\circ}\text{C}$.

4.3.2 Two-Color Solutions with Measured Emittance

Use of the measured spectral emittance values also causes the two-color measurement error (with no reflection) to approach zero, as would be expected if the emittances were precisely known. The two-color method, however, remains highly sensitive to the effects of reflected radiation with errors increasing to 60°C at 15-percent reflected energy.

4.3.3 Three-Color Solutions with Measured Emittance

Errors in the three-color solution using measured emittance values should also approach zero, but were 7°C without reflection. This illustrates that the two-color method (by virtue of its simplicity) is superior to the three-color method for the case where emittance ratios are precisely known, and where no incident radiation is present. The three-color measurement errors increased with increasing reflected energy, as did the two-color and the single-color errors. The three-color measurement errors with incident radiation are about the same order of magnitude as those for the single-color solution. But note that the three-color errors are dramatically reduced over the two-color errors. This indicates that the fundamental concept of the three-color solution is valid, provided that the necessary assumptions are met. While the three-color method does not appear to yield significantly better results than the single-color method in this experiment, one should remember that the single-color solutions represented in Fig. 21 require precise values of ϵ_1 , ϵ_2 , and ϵ_3 , while the three-color solution requires only that the emittance ratios be known. This means that if a truly gray target surface were used, the three-color method would yield good results without detailed information about spectral emittance.

5.0 CONCLUSIONS AND RECOMMENDATIONS

5.1 CONCLUSIONS

The objective of the experiment was to demonstrate an infrared surface temperature measurement technique that could be used without detailed prior knowledge of surface properties and could correct for errors that might be caused by incident radiation. The results discussed herein lead to the following conclusions:

1. The three-color solution errors in this experiment did not meet the goal of temperature measurements within ± 5 percent of the true temperature when incident radiation is present and when the gray-body assumption was used.
2. The three-color solution errors did not decrease significantly with the use of emittance estimates from published sources.

3. The three-color solution errors were less than 10°C (2 percent) when measured values of emittance were used to adjust the data. The measured values were derived from data collected with no incident radiation on the target surface. The requirement to collect data without incident radiation does not meet the objective of the three-color method. However, the positive results with the measured emittance values suggest that the three-color method may provide acceptable results on surfaces that more closely approximate gray-body behavior. Good results will also be possible if surface properties are known.
4. The two-color solution is highly sensitive to reflection of incident radiation, as anticipated. Measurement errors with measured values of emittance increased from less than 1°C with no reflection, to 60°C at 15-percent reflected energy (the maximum level of incident radiation experienced during the experiment).
5. The single-color solution is less sensitive to errors attributable to incident radiation than the two-color solution. The single-color solution errors with measured values of emittance are the same order of magnitude (less than 10°C) as the three-color solution errors.

5.2 RECOMMENDATIONS

The three-color measurement errors attributable to non-gray-body behavior may be reduced with corrections made possible by *a priori* surface property information in the form of room temperature target emittance and reflectance. The sensitivity to non-gray behavior can also be reduced by minimizing the spectral separation of the radiance ratios (minimize $(\lambda_2 - \lambda_1)$).

5.2.1 Further Investigations

Further investigations should include the following:

1. Investigate optimum spectral separation for radiance ratios used in the three-color technique.
2. The use of a circular variable filter in future experiments will allow the flexibility of selecting optimum radiance ratios for a given situation and may allow extension of the three-color technique to n-colors.
3. Further corrections to the data reported herein may be possible if bidirectional reflectance measurements are made of the target at room temperature.

5.2.2 Future Applications

While the results of this experiment indicate that single-color measurements may be as well suited as three-color measurements to situations with significant incident radiation, other factors such as a field of view that cannot be filled or radiance attenuation due to smoke, dust, or water vapor may dictate ratio pyrometry. For ratio pyrometry applications, the three-color method has been demonstrated to reduce the errors caused by incident radiation. Possible future applications in turbine engines might include the following:

1. Turbine engine hotparts — The internal surfaces of a typical turbine engine exhaust system (designated "hotparts") are much more complex than the geometry used for the demonstration of the three-color technique. Further study will be required to determine the suitability of the three-color technique to complex geometries with multiple sources of incident radiation.
2. Turbine engine pyrometry — The first row of turbine blades downstream of an annular combustor are subject to significant incident radiation. The turbine blade geometry is not significantly more complex than the simple geometry used in this experiment. The rotational speeds of the turbine blades will require pyrometer response times on the order of a microsecond (10^{-6} sec) (Ref. 7). Further study will be required to determine if such a high-response three-color pyrometer is feasible.

REFERENCES

1. DeWitt, D.P. and Kunz H. *Temperature, Its Measurement and Control in Science and Industry*, (Instrument Society of America, 1972), Vol. 4, Part 1, p. 600.
2. Holman, J.P. *Experimental Methods for Engineers*. McGraw-Hill Book Company, New York, 1978.
3. Atkinson, W. H. and Strange, R. R. "Pyrometer Temperature Measurements in the Presence of Reflected Radiation." Presented at the ASME-AIChE Heat Transfer Conference, St. Louis, MO, August 1976.
4. Atkinson, W. H. and Strange, R. R. "Turbine Pyrometry for Advanced Engines." Presented at the AIAA/SAE/ASME/ASCE 23rd Joint Propulsion Conference, San Diego, CA, June 29-July 2, 1987.

5. Hunter, G. B. , Allemand, C. D., and Edgar, T. W. "Multiwavelength Pyrometry: An Improved Method." *Optical Engineering*, Vol. 24, No. 6, November/December 1985, pp. 1081-1085.
6. "Thermal Radiation Properties Survey." Honeywell Research Center, Minneapolis-Honeywell Regulator Company, Minneapolis, MN., 1960.
7. Beynon, T.G.R. *Temperature, Its Measurement and Control in Science and Industry*, American Institute of Physics, 1982, Vol. 5, Part 1, p. 473.

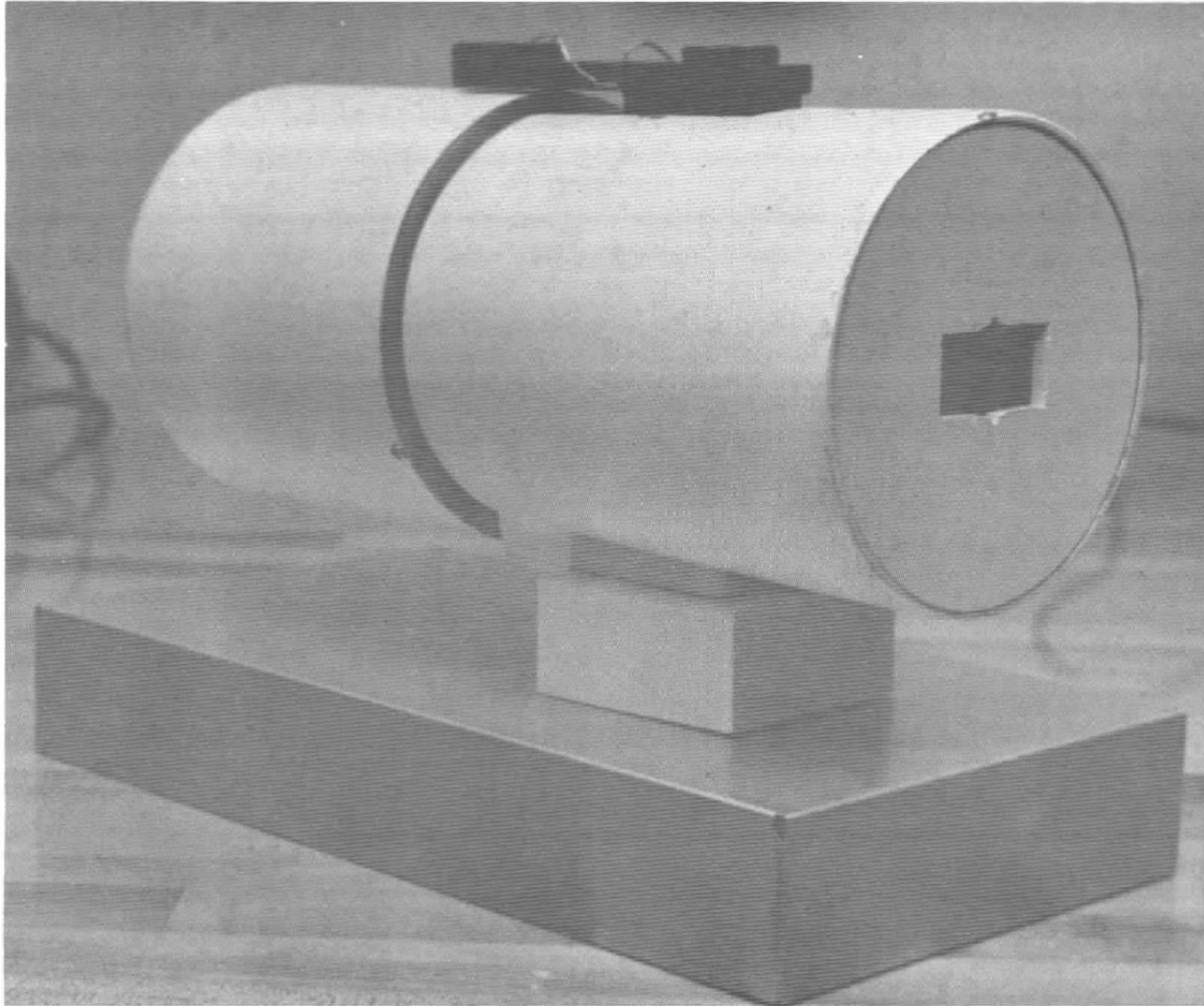


Figure 1. Barnes® spectral master radiometer.

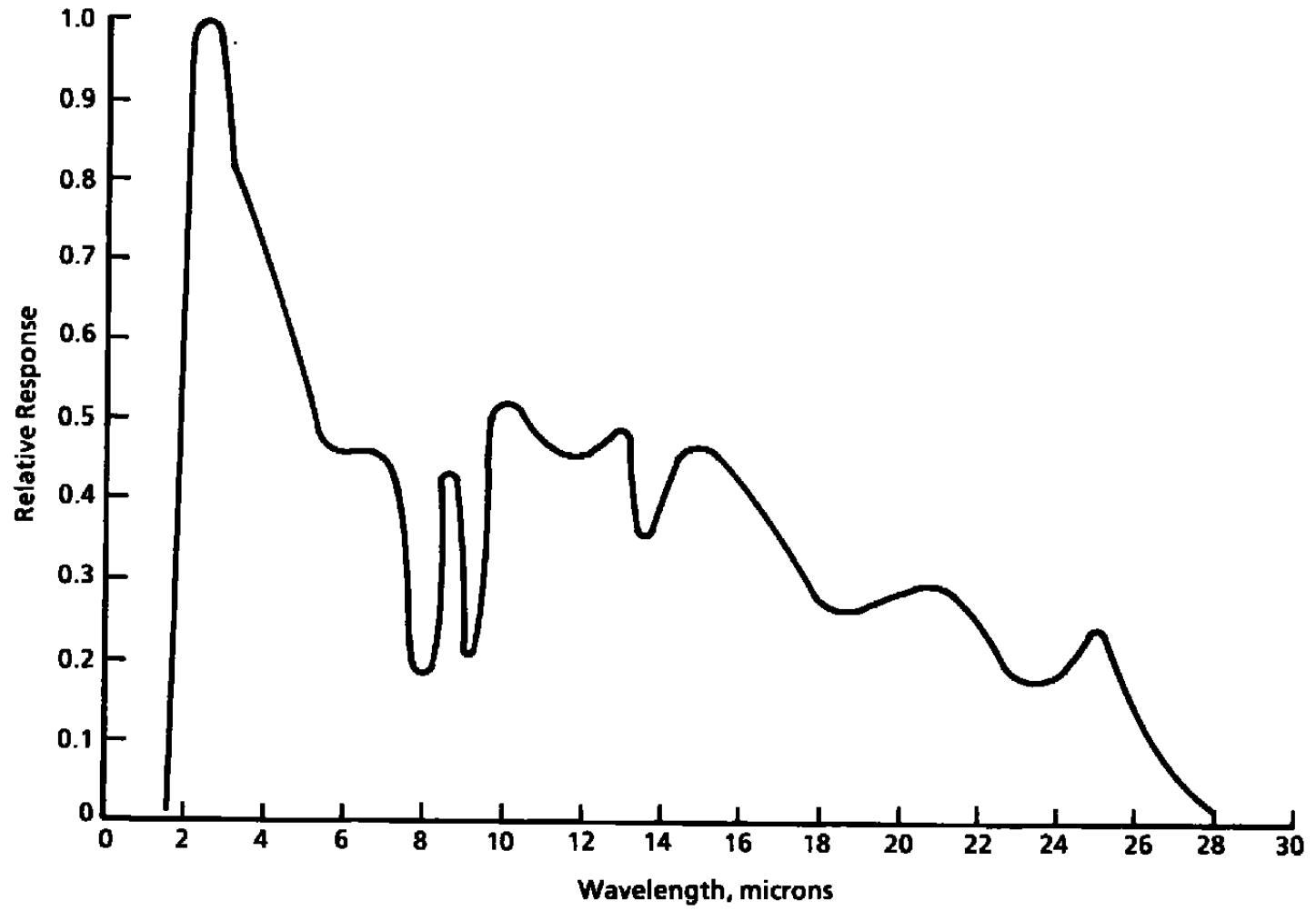


Figure 2. Barnes radiometer detector spectral response.

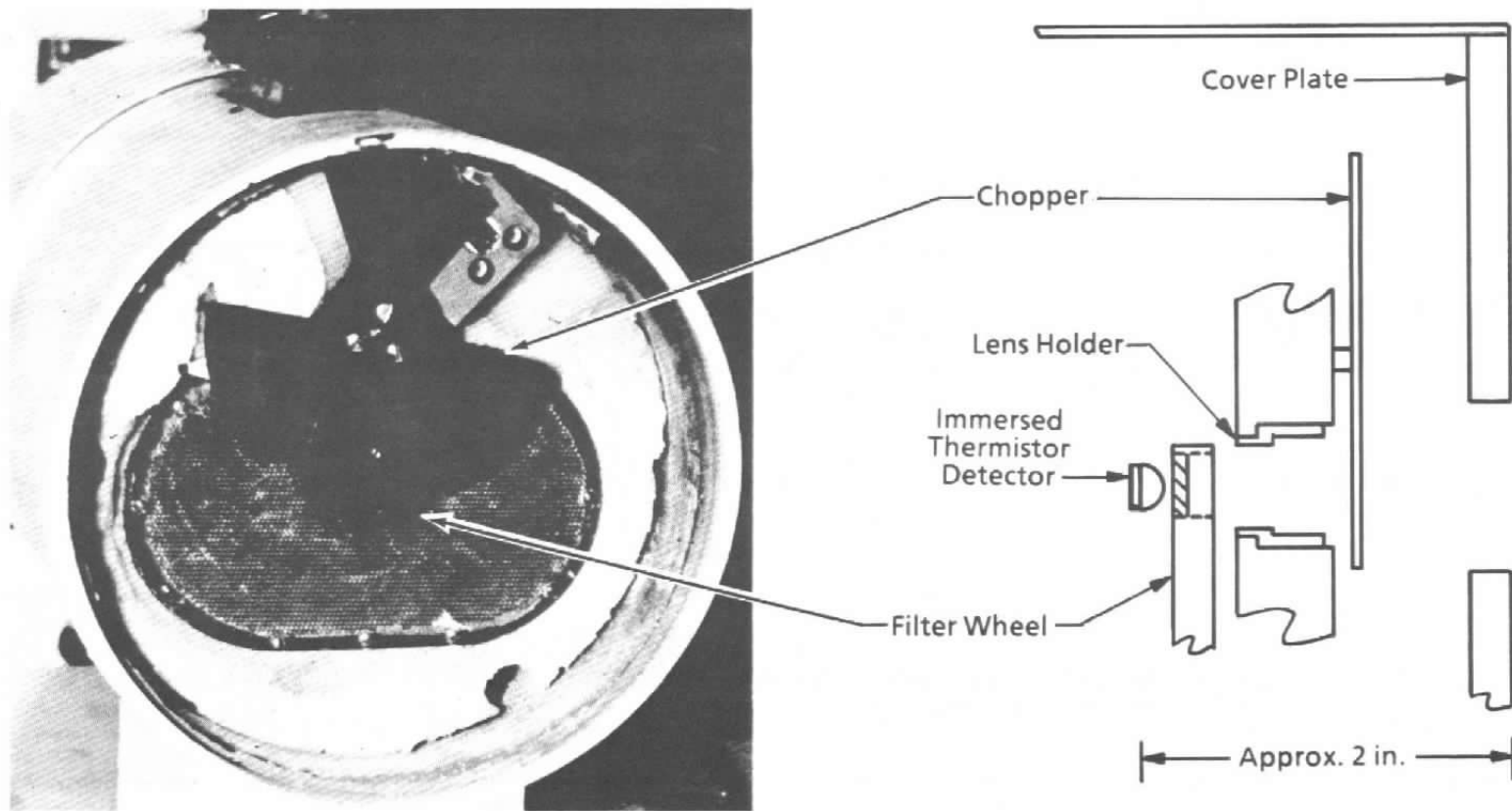


Figure 3. Internal view of Barnes spectral master radiometer.

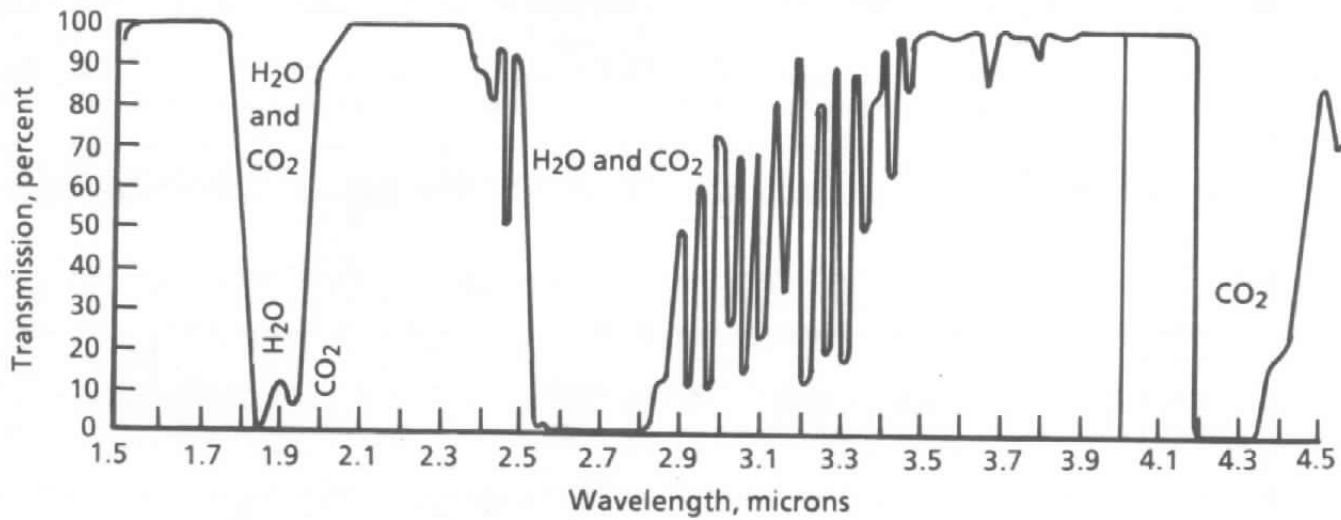


Figure 4. Water vapor and carbon dioxide absorption and emission bands in the 1.5- to 4.5- μ m range.

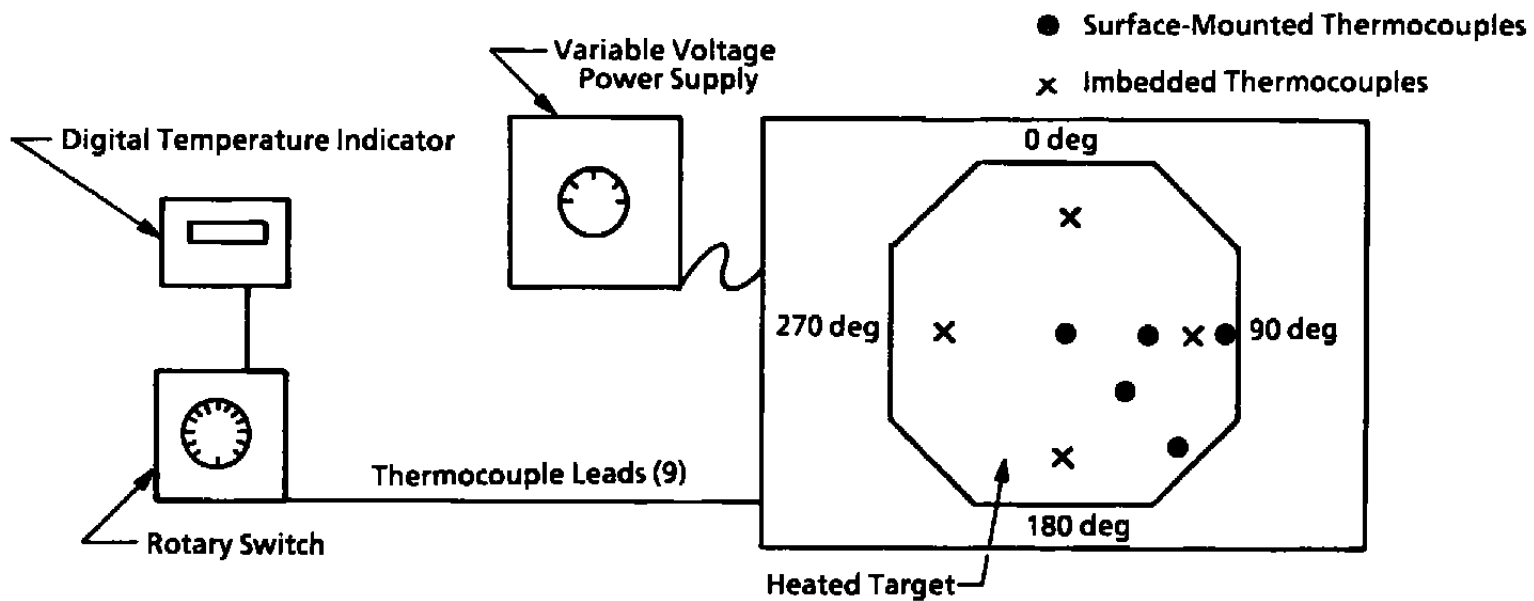


Figure 5. Electrically heated target surface.

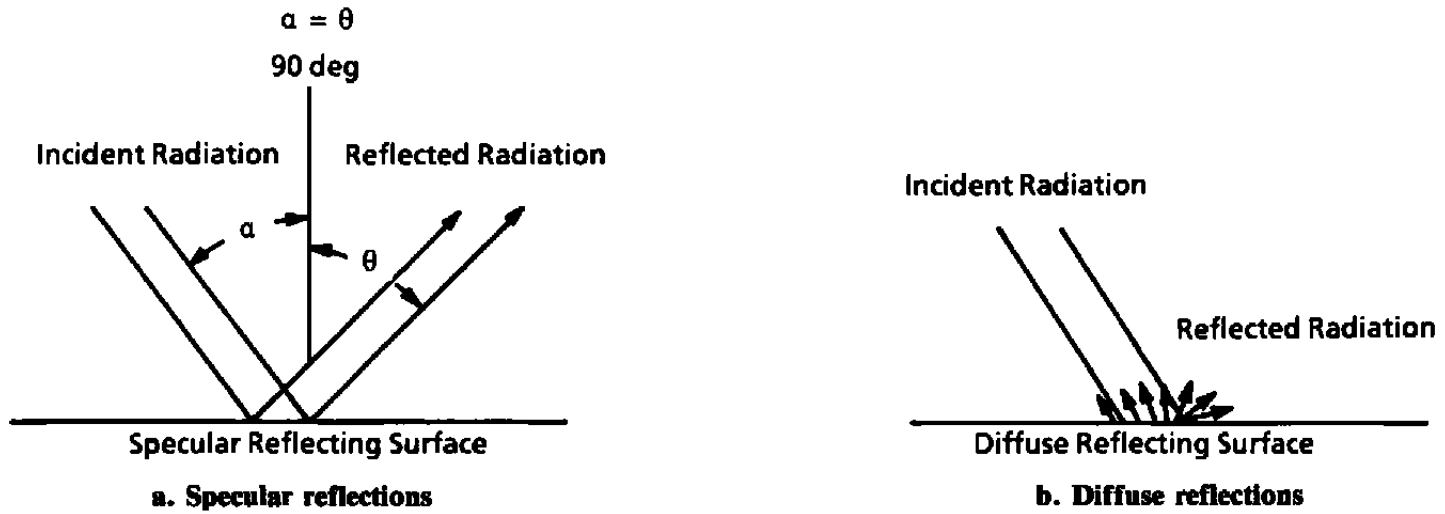


Figure 6. Comparison of specular and diffuse reflections.

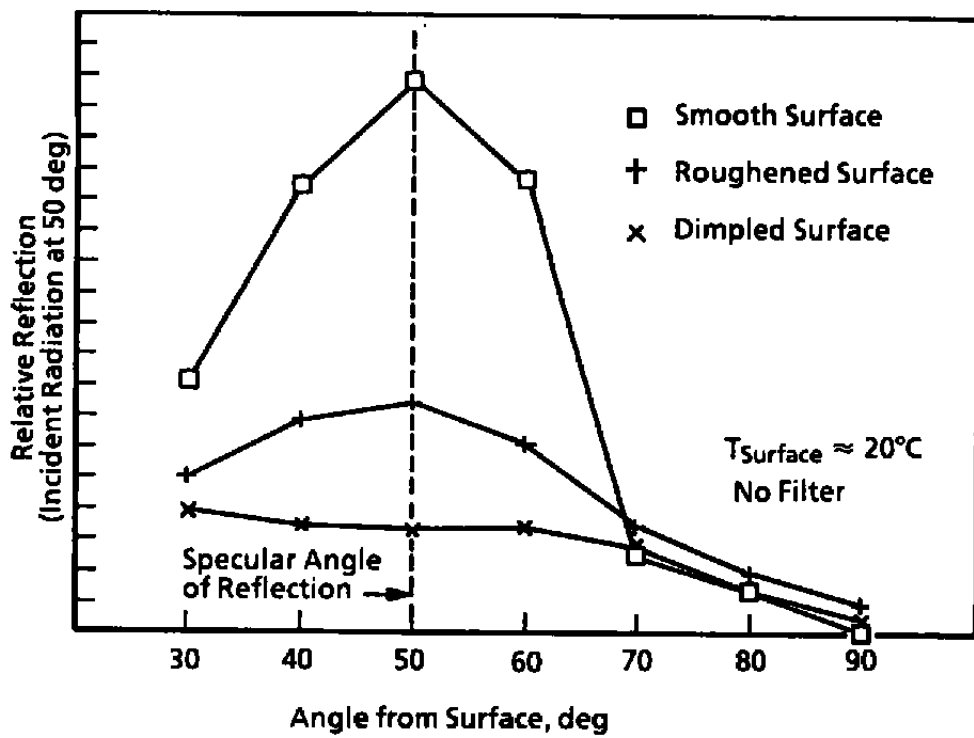
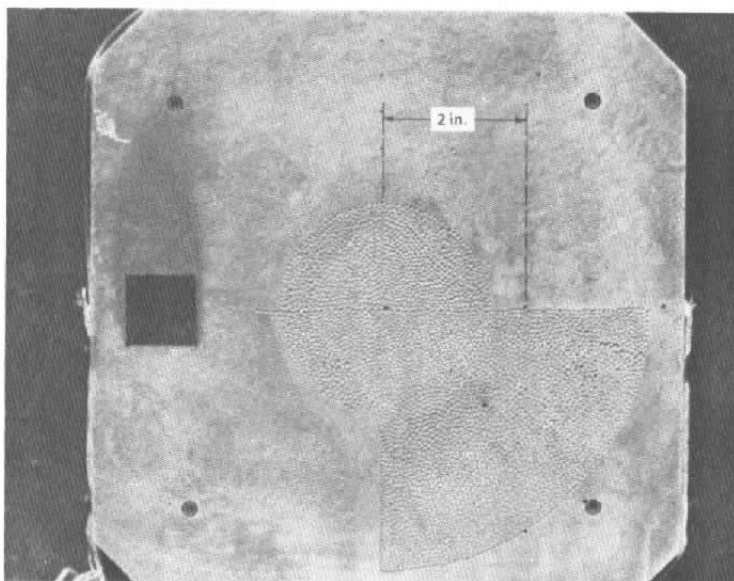
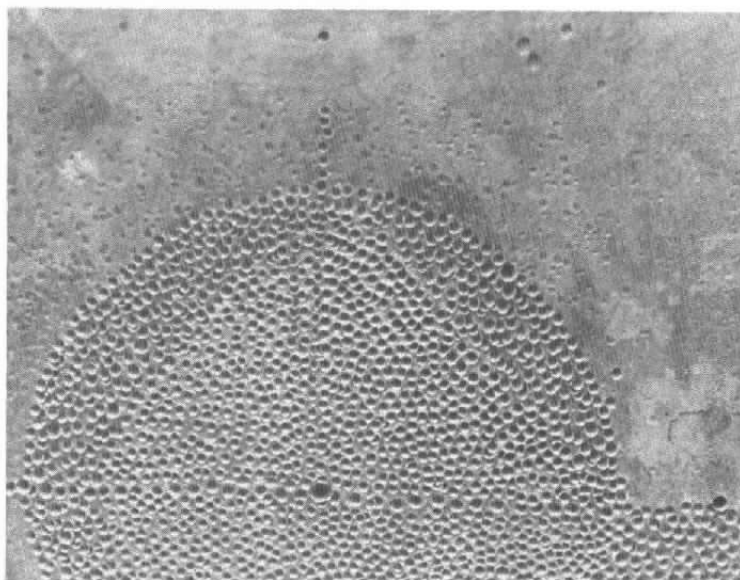


Figure 7. Target surface reflection characteristics before and after surface treatments.



a. Target



b. Close-up view of dimples

Figure 8. Aluminum target surface with dimples.

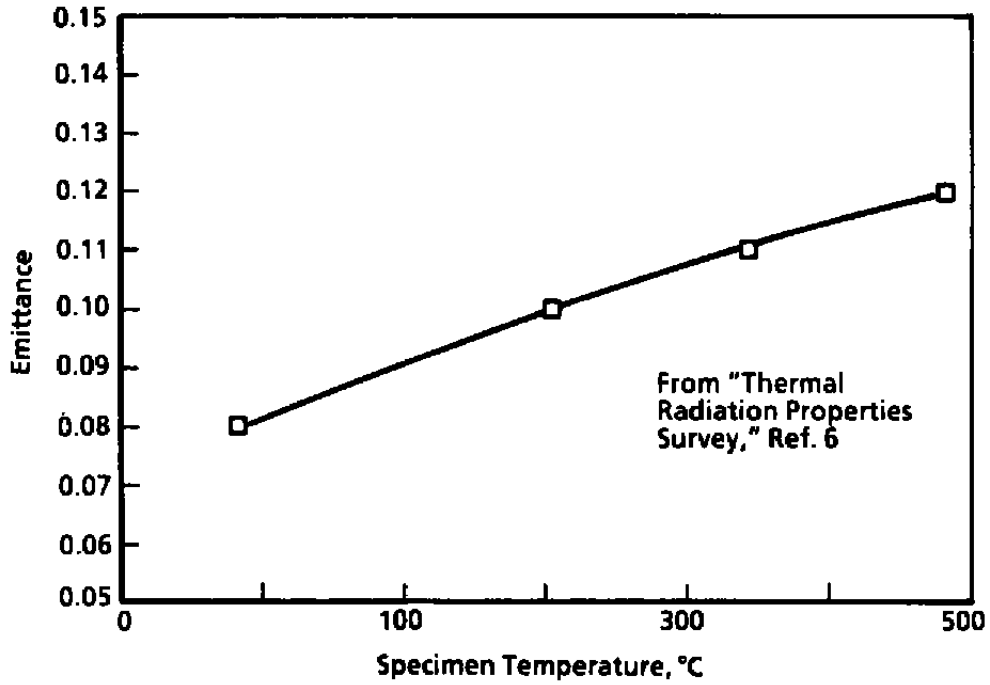


Figure 9. Total emittance of an aluminum plate (typical published values).

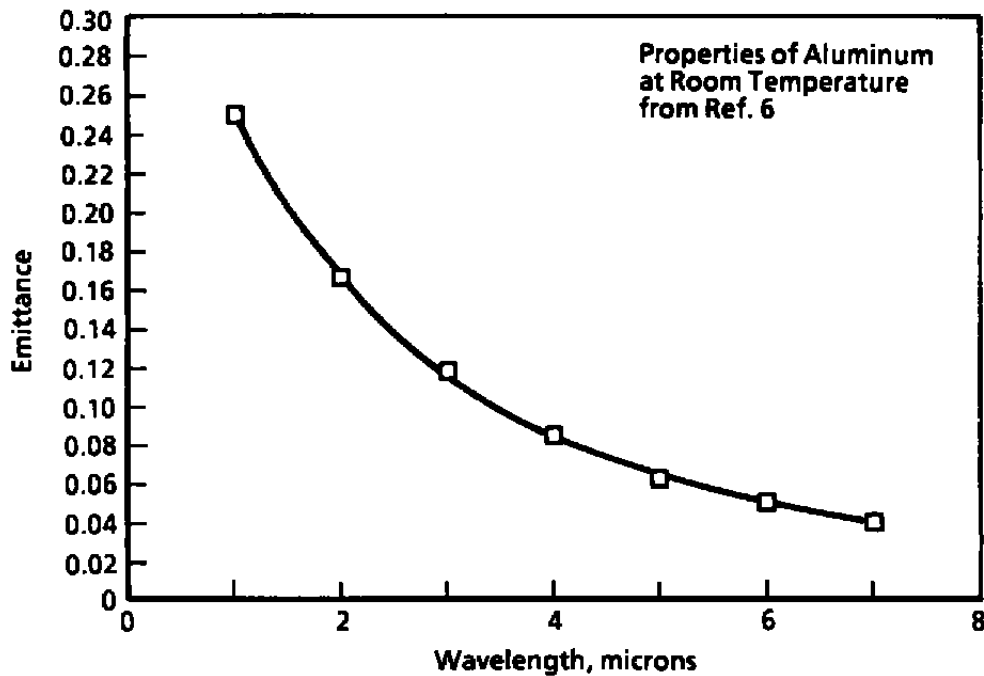


Figure 10. Spectral emittance of aluminum at room temperature (typical published values).

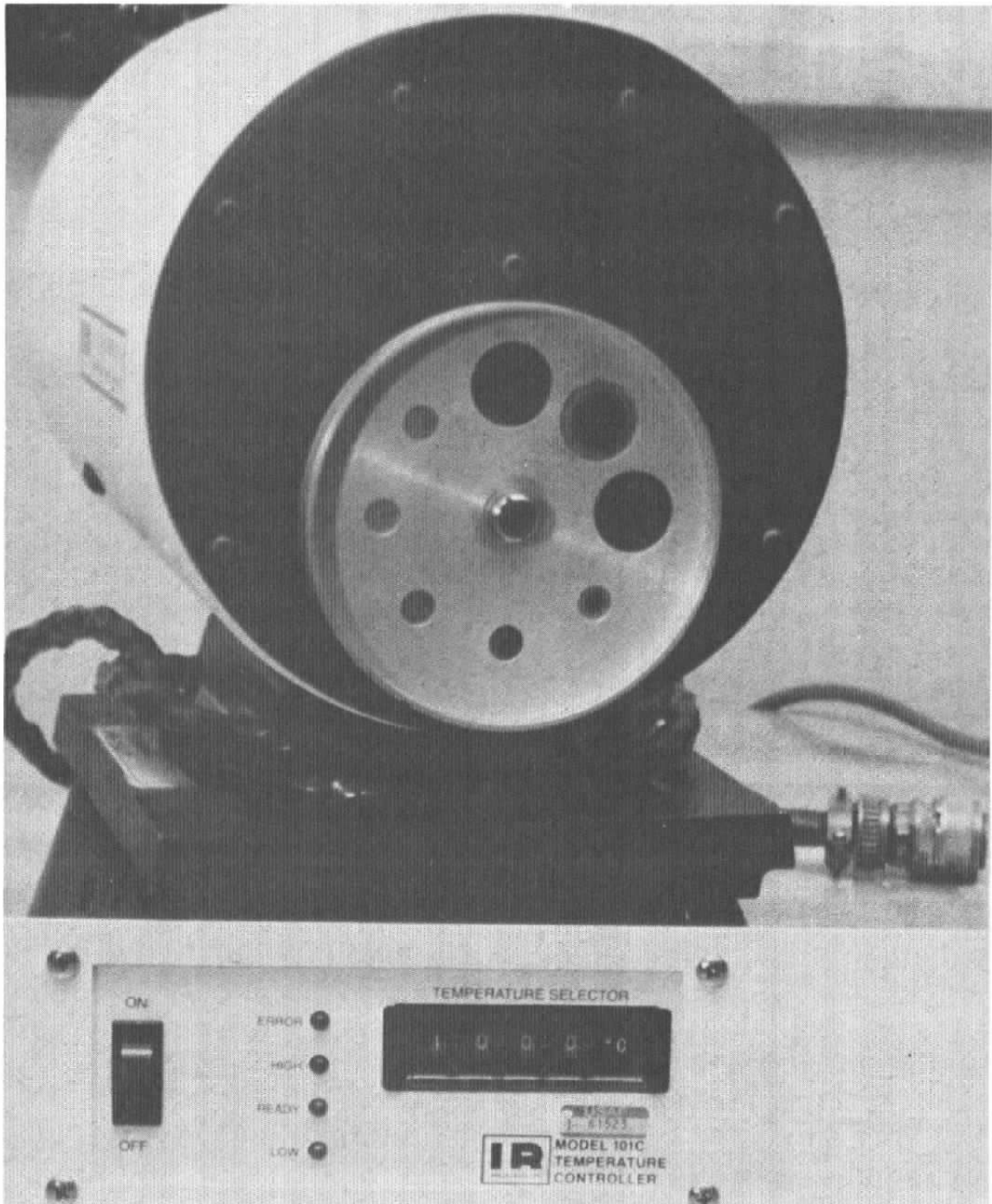


Figure 11. Photograph of 1-in. blackbody radiator.

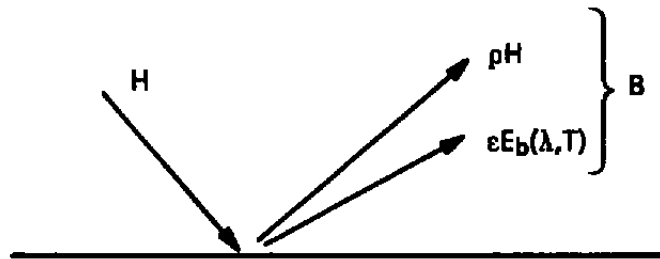


Figure 12. Radiosity (B).

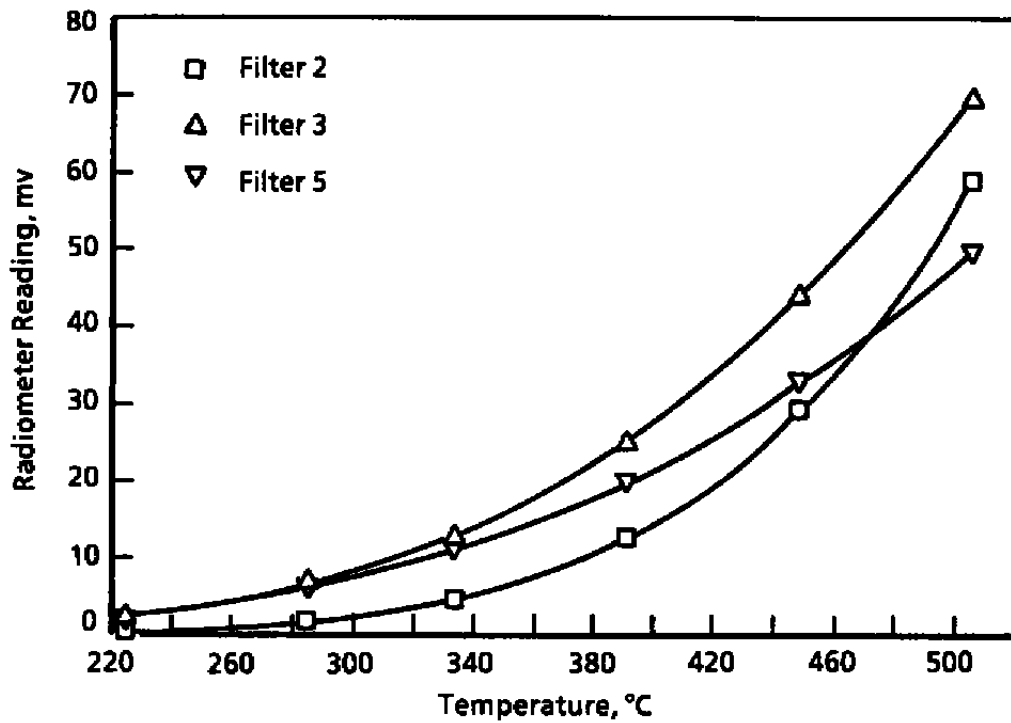


Figure 13. Single-color calibrations.

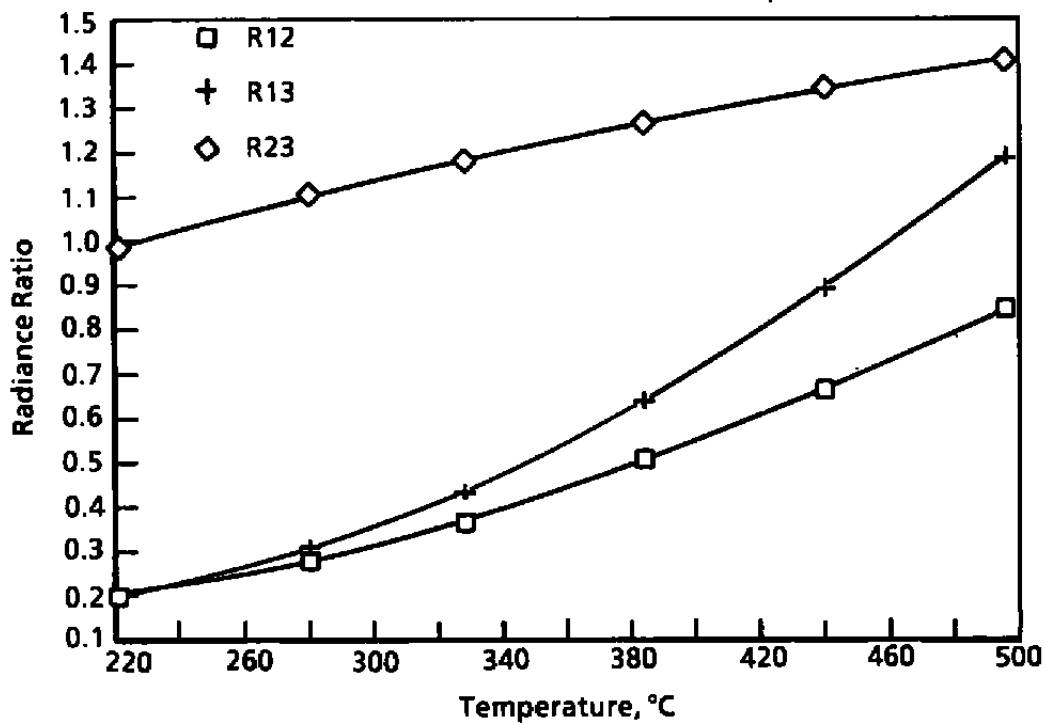
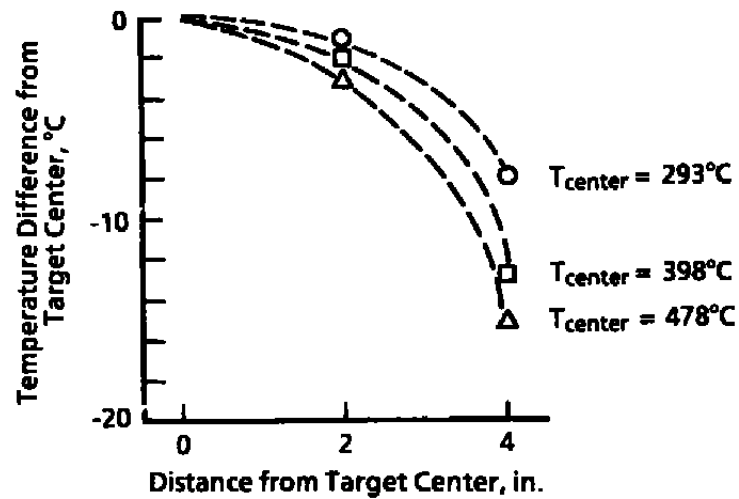
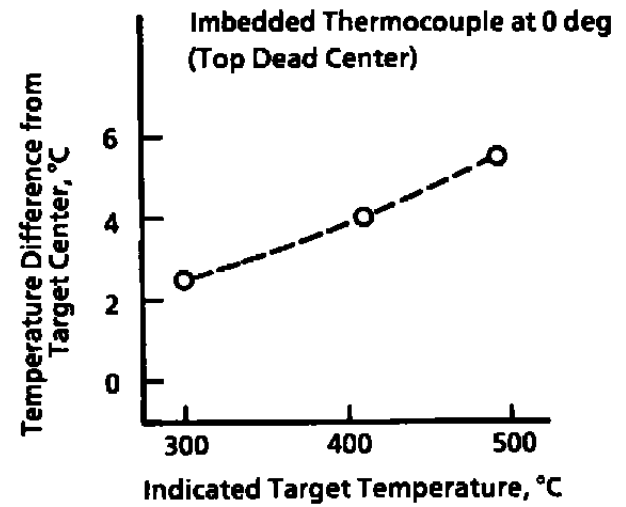


Figure 14. Radiance ratios.



a. Target radial profiles



b. Imbedded thermocouple correction

Figure 15. Target surface temperature profiles and correction to imbedded thermocouple readings.

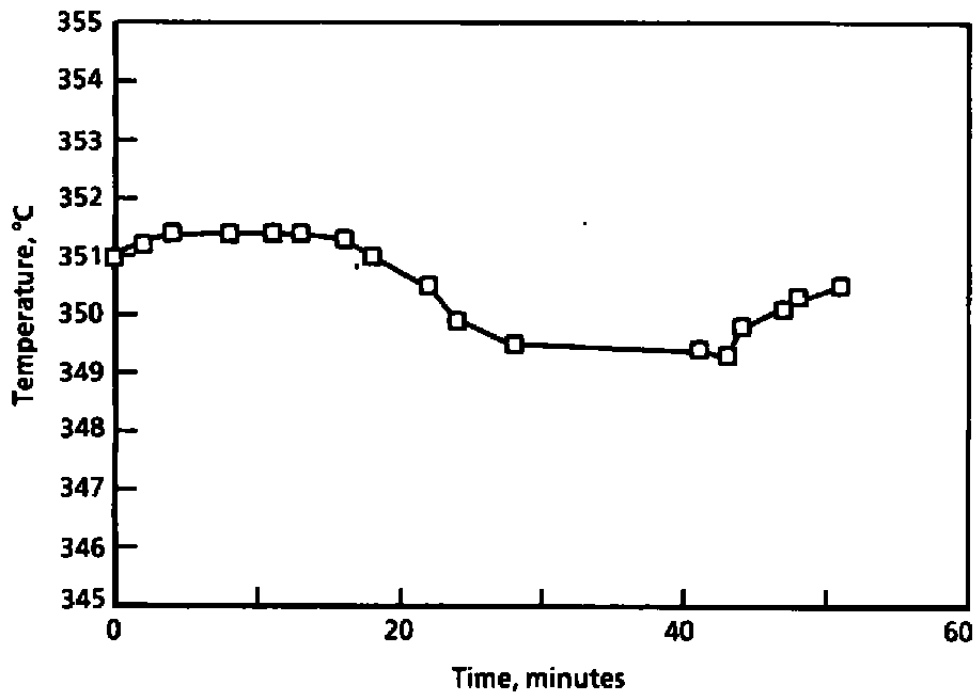


Figure 16. Target temperature stability during three-color experiment.

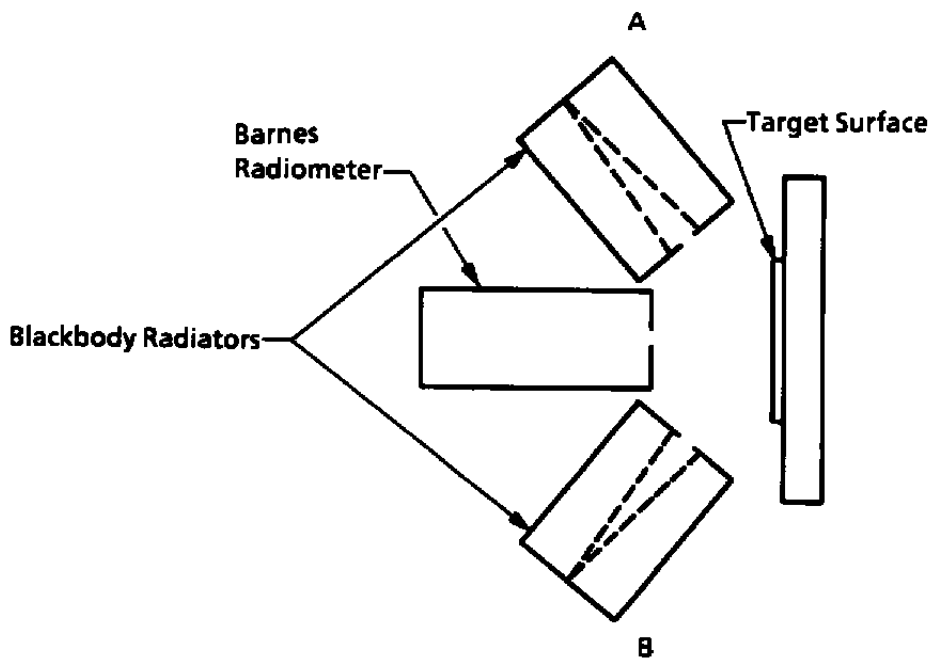
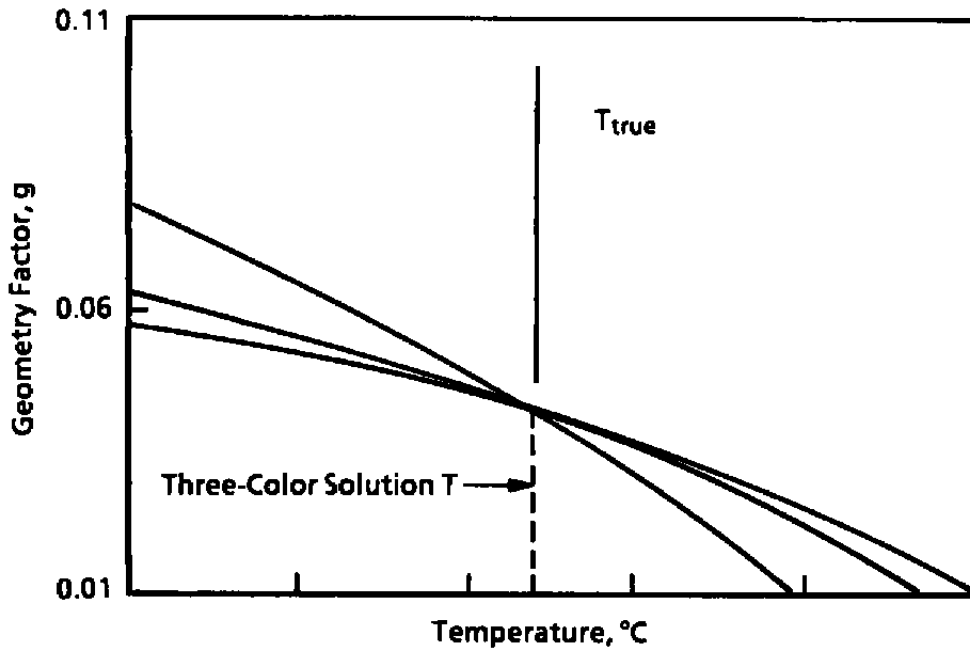
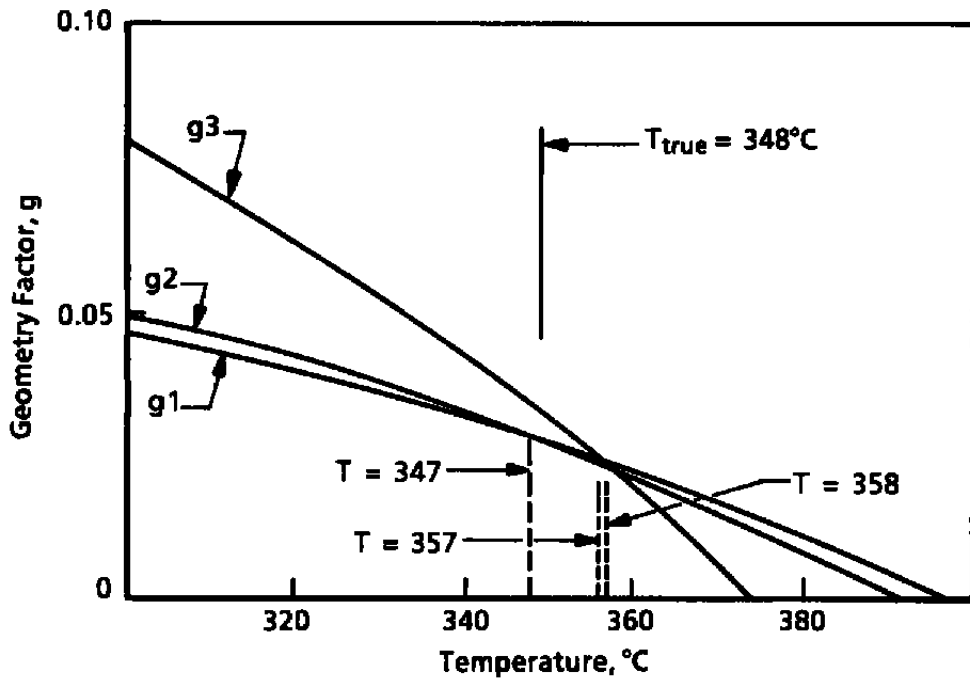


Figure 17. Hardware setup for three-color experiment.



a. Ideal solution (synthesized data)



b. Real solution (experimental data)

Figure 18. Geometry factor (g) convergence leading to three-color solutions.

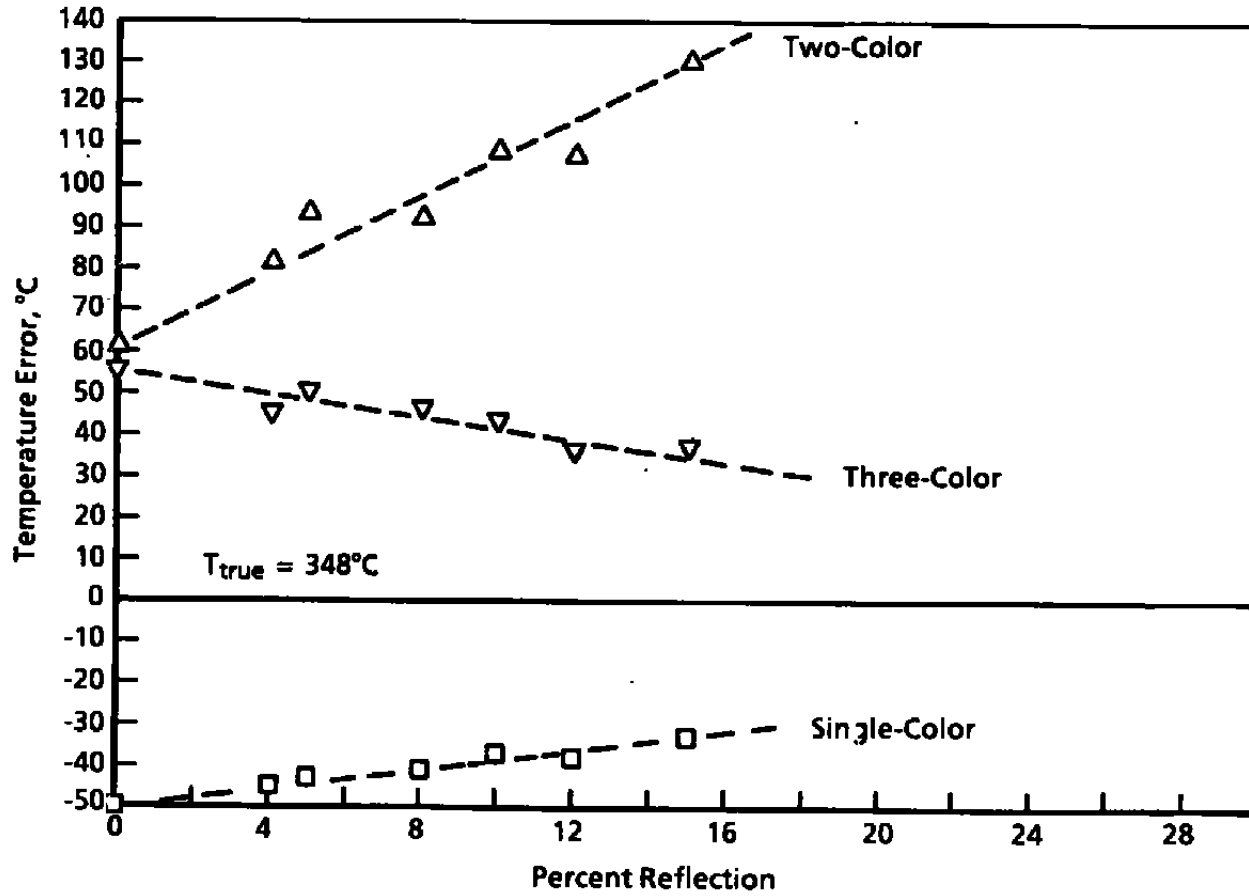


Figure 19. Comparison of calculated temperature errors with increasing reflected radiant energy (gray-body assumption).

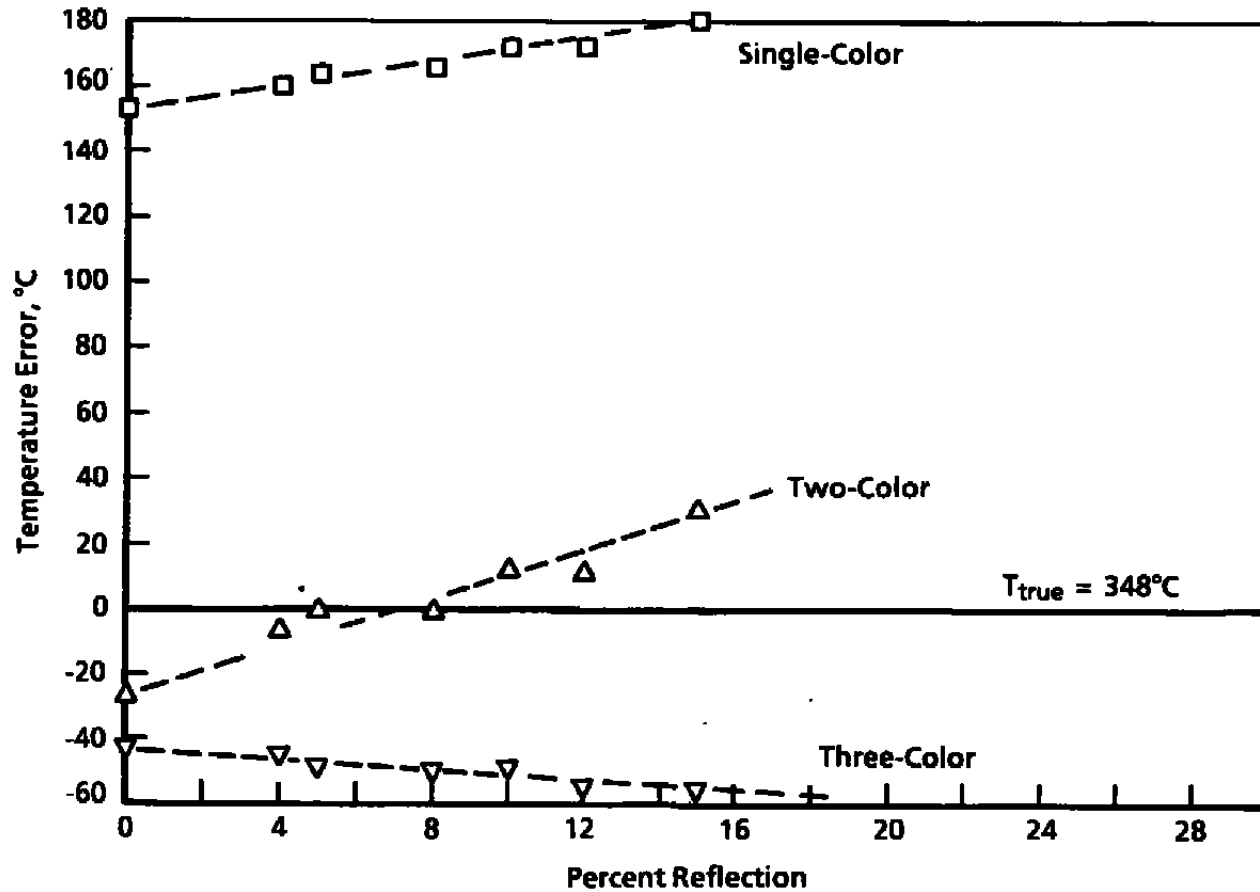


Figure 20. Comparison of calculated temperature errors with increasing reflected radiant energy (using published values for emittance).

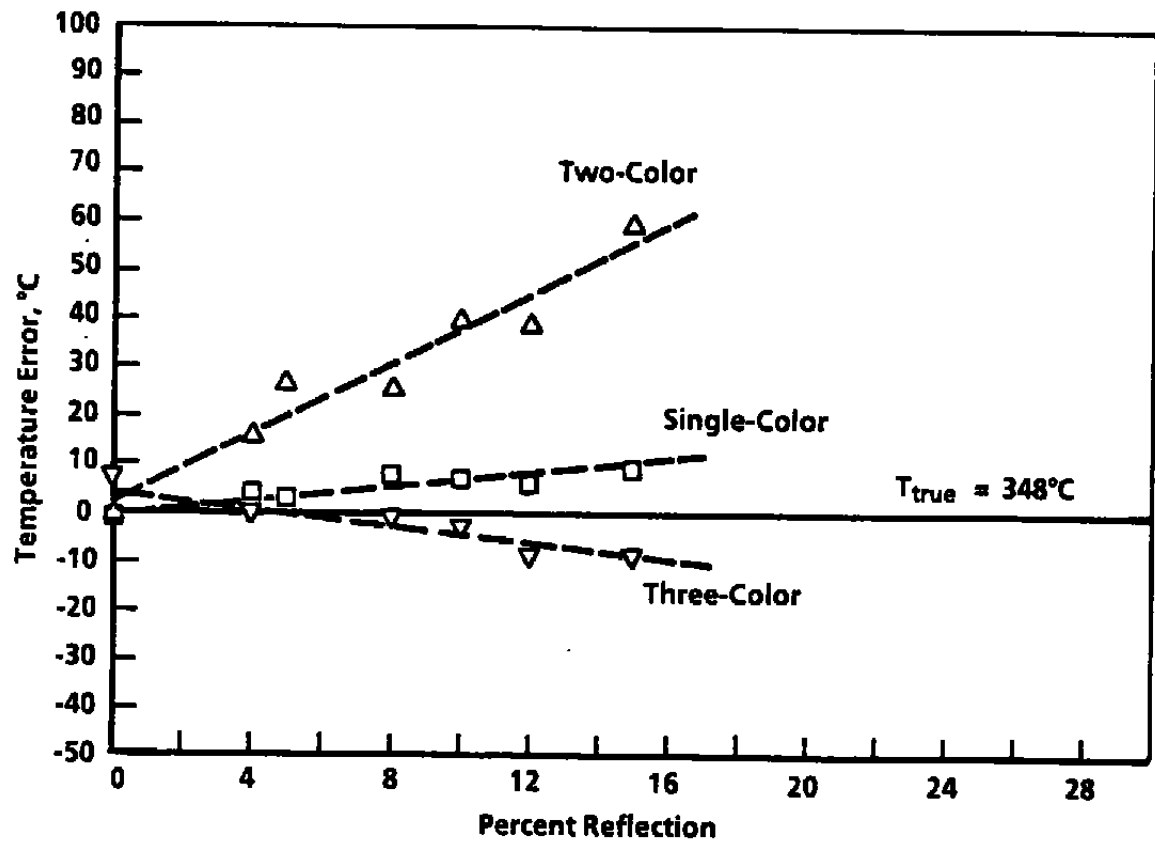


Figure 21. Comparison of calculated temperature errors with increasing reflected radiant energy (using measured values for emittance).

Table 1. List of Filters Installed in Barnes Radiometer

Wheel Position	Lower Half-Power Point, μm	Upper Half-Power Point, μm	Bandwidth, μm	Center Wavelength, μm
1	1.987	2.063	0.076	2.025
2	2.033	2.385	0.352	2.209
3	3.398	3.599	0.201	3.4985
4	3.398	3.670	0.272	3.534
5	3.807	3.969	0.161	3.888
6	3.939	4.105	0.166	4.022
7	9.948	11.428	1.480	10.688
8		No filter		

Table 2. Tabulated Radiance Ratios from 300 to 500°C

Temperature	R12	R13	R23
300	0.3059	0.3419	1.1194
301	0.3076	0.3444	1.1209
302	0.3094	0.3470	1.1225
303	0.3112	0.3495	1.1240
304	0.3130	0.3521	1.1256
305	0.3148	0.3547	1.1271
306	0.3166	0.3573	1.1287
307	0.3184	0.3599	1.1302
308	0.3202	0.3626	1.1318
309	0.3221	0.3652	1.1333
310	0.3239	0.3679	1.1349
311	0.3257	0.3706	1.1364
312	0.3276	0.3733	1.1380
313	0.3295	0.3760	1.1395
314	0.3313	0.3787	1.1410
315	0.3332	0.3815	1.1426
316	0.3351	0.3842	1.1441
317	0.3370	0.3870	1.1457
318	0.3389	0.3898	1.1472
319	0.3408	0.3926	1.1487
320	0.3428	0.3954	1.1503
321	0.3447	0.3983	1.1518
322	0.3466	0.4011	1.1533
323	0.3486	0.4040	1.1549
324	0.3505	0.4069	1.1564
325	0.3525	0.4098	1.1579
326	0.3545	0.4127	1.1595
327	0.3565	0.4156	1.1610
328	0.3585	0.4186	1.1625
329	0.3605	0.4215	1.1640
330	0.3625	0.4245	1.1656
331	0.3645	0.4275	1.1671
332	0.3665	0.4305	1.1686
333	0.3686	0.4336	1.1701
334	0.3706	0.4366	1.1717
335	0.3726	0.4397	1.1732
336	0.3747	0.4427	1.1747
337	0.3768	0.4458	1.1762
338	0.3789	0.4489	1.1777
339	0.3809	0.4521	1.1793
340	0.3830	0.4552	1.1808
341	0.3851	0.4583	1.1823
342	0.3872	0.4615	1.1838
343	0.3894	0.4647	1.1853
344	0.3915	0.4679	1.1868
345	0.3936	0.4711	1.1883
346	0.3958	0.4743	1.1899
347	0.3979	0.4776	1.1914
348	0.4001	0.4809	1.1929
349	0.4023	0.4841	1.1944
350	0.4044	0.4874	1.1959

Table 2. Continued

Temperature	R12	R13	R23
351	0.4066	0.4907	1.1974
352	0.4088	0.4941	1.1989
353	0.4110	0.4974	1.2004
354	0.4132	0.5008	1.2019
355	0.4155	0.5041	1.2034
356	0.4177	0.5075	1.2049
357	0.4199	0.5109	1.2064
358	0.4222	0.5143	1.2079
359	0.4244	0.5178	1.2094
360	0.4267	0.5212	1.2109
361	0.4290	0.5247	1.2124
362	0.4313	0.5282	1.2139
363	0.4335	0.5317	1.2154
364	0.4358	0.5352	1.2169
365	0.4381	0.5387	1.2183
366	0.4405	0.5423	1.2198
367	0.4428	0.5458	1.2213
368	0.4451	0.5494	1.2228
369	0.4475	0.5530	1.2243
370	0.4498	0.5566	1.2258
371	0.4522	0.5602	1.2273
372	0.4545	0.5639	1.2288
373	0.4569	0.5675	1.2302
374	0.4593	0.5712	1.2317
375	0.4617	0.5749	1.2332
376	0.4641	0.5786	1.2347
377	0.4665	0.5823	1.2362
378	0.4689	0.5860	1.2376
379	0.4713	0.5898	1.2391
380	0.4738	0.5935	1.2406
381	0.4762	0.5973	1.2421
382	0.4786	0.6011	1.2435
383	0.4811	0.6049	1.2450
384	0.4836	0.6088	1.2465
385	0.4860	0.6126	1.2480
386	0.4885	0.6165	1.2494
387	0.4910	0.6203	1.2509
388	0.4935	0.6242	1.2524
389	0.4960	0.6281	1.2538
390	0.4986	0.6320	1.2553
391	0.5011	0.6360	1.2568
392	0.5036	0.6399	1.2582
393	0.5062	0.6439	1.2597
394	0.5087	0.6479	1.2611
395	0.5113	0.6519	1.2626
396	0.5138	0.6559	1.2641
397	0.5164	0.6599	1.2655
398	0.5190	0.6640	1.2670
399	0.5216	0.6680	1.2684
400	0.5242	0.6721	1.2699

Table 2. Continued

Temperature	R12	R13	R23
401	0.5268	0.6762	1.2713
402	0.5294	0.6803	1.2728
403	0.5321	0.6844	1.2743
404	0.5347	0.6886	1.2757
405	0.5373	0.6927	1.2772
406	0.5400	0.6969	1.2786
407	0.5427	0.7011	1.2801
408	0.5453	0.7053	1.2815
409	0.5480	0.7095	1.2830
410	0.5507	0.7137	1.2844
411	0.5534	0.7180	1.2858
412	0.5561	0.7223	1.2873
413	0.5588	0.7265	1.2887
414	0.5615	0.7308	1.2902
415	0.5643	0.7352	1.2916
416	0.5670	0.7395	1.2930
417	0.5697	0.7438	1.2945
418	0.5725	0.7482	1.2959
419	0.5753	0.7526	1.2974
420	0.5780	0.7569	1.2988
421	0.5808	0.7614	1.3002
422	0.5836	0.7658	1.3017
423	0.5864	0.7702	1.3031
424	0.5892	0.7747	1.3045
425	0.5920	0.7791	1.3060
426	0.5948	0.7836	1.3074
427	0.5977	0.7881	1.3088
428	0.6005	0.7926	1.3102
429	0.6034	0.7972	1.3117
430	0.6062	0.8017	1.3131
431	0.6091	0.8063	1.3145
432	0.6120	0.8109	1.3159
433	0.6148	0.8155	1.3174
434	0.6177	0.8201	1.3188
435	0.6206	0.8247	1.3202
436	0.6235	0.8293	1.3216
437	0.6265	0.8340	1.3231
438	0.6294	0.8387	1.3245
439	0.6323	0.8433	1.3259
440	0.6353	0.8481	1.3273
441	0.6382	0.8528	1.3287
442	0.6412	0.8575	1.3301
443	0.6441	0.8623	1.3315
444	0.6471	0.8670	1.3330
445	0.6501	0.8718	1.3344
446	0.6531	0.8766	1.3358
447	0.6561	0.8814	1.3372
448	0.6591	0.8862	1.3386
449	0.6621	0.8911	1.3400
450	0.6651	0.8960	1.3414

Table 2. Concluded

Temperature	R12	R13	R23
451	0.6682	0.9008	1.3428
452	0.6712	0.9057	1.3442
453	0.6743	0.9106	1.3456
454	0.6773	0.9156	1.3470
455	0.6804	0.9205	1.3484
456	0.6835	0.9254	1.3498
457	0.6866	0.9304	1.3512
458	0.6897	0.9354	1.3526
459	0.6928	0.9404	1.3540
460	0.6959	0.9454	1.3554
461	0.6990	0.9505	1.3568
462	0.7021	0.9555	1.3582
463	0.7053	0.9606	1.3596
464	0.7084	0.9656	1.3610
465	0.7116	0.9707	1.3624
466	0.7147	0.9758	1.3638
467	0.7179	0.9810	1.3651
468	0.7211	0.9861	1.3665
469	0.7243	0.9913	1.3679
470	0.7275	0.9965	1.3693
471	0.7307	1.0016	1.3707
472	0.7339	1.0068	1.3721
473	0.7371	1.0121	1.3735
474	0.7403	1.0173	1.3748
475	0.7436	1.0226	1.3762
476	0.7468	1.0278	1.3776
477	0.7501	1.0331	1.3790
478	0.7533	1.0384	1.3804
479	0.7566	1.0437	1.3817
480	0.7599	1.0490	1.3831
481	0.7632	1.0544	1.3845
482	0.7665	1.0598	1.3859
483	0.7698	1.0651	1.3872
484	0.7731	1.0705	1.3886
485	0.7764	1.0759	1.3900
486	0.7798	1.0814	1.3913
487	0.7831	1.0868	1.3927
488	0.7864	1.0923	1.3941
489	0.7898	1.0977	1.3954
490	0.7932	1.1032	1.3968
491	0.7965	1.1087	1.3982
492	0.7999	1.1142	1.3995
493	0.8033	1.1198	1.4009
494	0.8067	1.1253	1.4023
495	0.8101	1.1309	1.4036
496	0.8135	1.1365	1.4050
497	0.8170	1.1421	1.4063
498	0.8204	1.1477	1.4077
499	0.8238	1.1533	1.4091
500	0.8273	1.1589	1.4104

Table 3. Estimated Contributors to Target Surface Temperature Uncertainty

Source of Uncertainty	Estimated Contribution (less than or equal to)
Thermocouple Reading	$\pm 3^{\circ}\text{C}$
Radiation Error on Thermocouple	$\pm 2^{\circ}\text{C}$
Radial Temperature Profile	$\pm 1^{\circ}\text{C}$
Circumferential Temperature Profile	$\pm 2^{\circ}\text{C}$
Effect of Dimples	$\pm 1^{\circ}\text{C}$
Temperature Fluctuation with Time	$\pm 1^{\circ}\text{C}$
Unaccounted For (Miscellaneous)	$\pm 2^{\circ}\text{C}$
Cumulative (Root sum of squares)	$\pm 5^{\circ}\text{C}$

Table 4. Summary of Single-Color, Two-Color, and Three-Color Solutions with Gray-Body Behavior

Percent Reflected Energy	Gray-Body Assumption Calculated Temperatures		
	1-Color Solution, $^{\circ}\text{C}$	2-Color Solution, $^{\circ}\text{C}$	3-Color Solution, $^{\circ}\text{C}$
0	298	410	403
4	303	430	393
8	307	441	394
12	310	456	384
5	305	442	398
10	311	457	391
15	315	479	385

Table 5. Summary of Single-Color, Two-Color, and Three-Color Solutions with Published Values for Emittance

Percent Reflected Energy	Calculated Temperatures		
	1-Color Solution, °C	2-Color Solution, °C	3-Color Solution, °C
0	501	322	305
4	508	342	303
8	514	348	298
12	520	360	293
5	512	348	299
10	520	361	299
15	528	379	292

Table 6. Summary of Single-Color, Two-Color, and Three-Color Solutions with Measured Values for Emittance

Percent Reflected Energy	Calculated Temperatures		
	1-Color Solution, °C	2-Color Solution, °C	3-Color Solution, °C
0	347	348	355
4	352	364	348
8	356	374	347
12	354	387	339
5	351	375	350
10	355	388	345
15	357	408	339